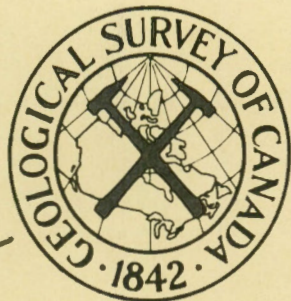


~~MS~~

MSC

Paper

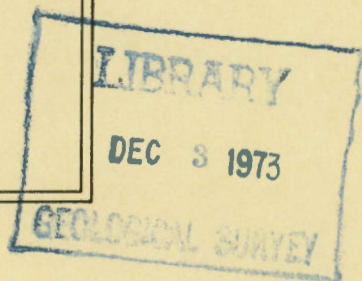
73-25



GEOLOGICAL  
SURVEY  
OF  
CANADA

PAPER 73-25

DEPARTMENT OF ENERGY,  
MINES AND RESOURCES



ELECTROMAGNETIC FIELDS OF OSCILLATING  
MAGNETIC DIPOLES PLACED OVER A  
MULTILAYER CONDUCTING EARTH

A. K. Sinha and L. S. Collett

This document was produced  
by scanning the original publication.

Ce document est le produit d'une  
numérisation par balayage  
de la publication originale.



**GEOLOGICAL SURVEY  
OF CANADA**

**PAPER 73-25**

**ELECTROMAGNETIC FIELDS OF OSCILLATING  
MAGNETIC DIPOLES PLACED OVER A  
MULTILAYER CONDUCTING EARTH**

**A. K. Sinha and L. S. Collett**

**DEPARTMENT OF ENERGY, MINES AND RESOURCES**

©Crown Copyrights reserved  
Available by mail from *Information Canada*, Ottawa

from the Geological Survey of Canada  
601 Booth St., Ottawa

and

*Information Canada* bookshops in

HALIFAX - 1687 Barrington Street  
MONTREAL - 640 St. Catherine Street W.  
OTTAWA - 171 Slater Street  
TORONTO - 221 Yonge Street  
WINNIPEG - 393 Portage Avenue  
VANCOUVER - 800 Granville Street

or through your bookseller

Price:\$2.00

Catalogue No.M44-73-25

Price subject to change without notice

*Information Canada*  
Ottawa  
1973

## CONTENTS

	Page														
Abstract/Résumé.....	v														
Introduction.....	1														
Mathematical development.....	2														
Description of the Program.....	10														
Results.....	12														
Concluding remarks .....	14														
Acknowledgments.....	28														
References .....	28														
Appendix I. Proof of minimum coupling between the coils in system 5 .....															
	30														
II. Computer program for determining the polarization characteristics of the E. M. fields due to airborne dipoles.....															
	31														
<u>Illustrations</u>															
Figure	<table style="width: 100%; border-collapse: collapse;"> <tbody> <tr> <td style="padding-left: 2em;">1. Magnetic dipole over an n-layer earth .....</td> <td style="text-align: right; vertical-align: bottom;">3</td> </tr> <tr> <td style="padding-left: 2em;">2. Tilt angle and ellipticity for an elliptically polarized field and parameters of the models con- sidered .....</td> <td style="text-align: right; vertical-align: bottom;">15</td> </tr> <tr> <td style="padding-left: 2em;">3- 8. Variations of the tilt angle and ellipticity with B for the form models of series 1.....</td> <td style="text-align: right; vertical-align: bottom;">16-18</td> </tr> <tr> <td style="padding-left: 2em;">9-14. Variation of the tilt angle and ellipticity with B for three values of A/B for the four models belonging to series 2 .....</td> <td style="text-align: right; vertical-align: bottom;">19-21</td> </tr> <tr> <td style="padding-left: 2em;">15-17. Variations of the tilt angle with B for the four models of series 1 .....</td> <td style="text-align: right; vertical-align: bottom;">22-23</td> </tr> <tr> <td style="padding-left: 2em;">18-20. Variations of the ellipticity with B for models of series 1 .....</td> <td style="text-align: right; vertical-align: bottom;">23-24</td> </tr> <tr> <td style="padding-left: 2em;">21-26. Variations of the ellipticity with B for models of series 2 .....</td> <td style="text-align: right; vertical-align: bottom;">25-27</td> </tr> </tbody> </table>	1. Magnetic dipole over an n-layer earth .....	3	2. Tilt angle and ellipticity for an elliptically polarized field and parameters of the models con- sidered .....	15	3- 8. Variations of the tilt angle and ellipticity with B for the form models of series 1.....	16-18	9-14. Variation of the tilt angle and ellipticity with B for three values of A/B for the four models belonging to series 2 .....	19-21	15-17. Variations of the tilt angle with B for the four models of series 1 .....	22-23	18-20. Variations of the ellipticity with B for models of series 1 .....	23-24	21-26. Variations of the ellipticity with B for models of series 2 .....	25-27
1. Magnetic dipole over an n-layer earth .....	3														
2. Tilt angle and ellipticity for an elliptically polarized field and parameters of the models con- sidered .....	15														
3- 8. Variations of the tilt angle and ellipticity with B for the form models of series 1.....	16-18														
9-14. Variation of the tilt angle and ellipticity with B for three values of A/B for the four models belonging to series 2 .....	19-21														
15-17. Variations of the tilt angle with B for the four models of series 1 .....	22-23														
18-20. Variations of the ellipticity with B for models of series 1 .....	23-24														
21-26. Variations of the ellipticity with B for models of series 2 .....	25-27														



## ABSTRACT

The electromagnetic fields from oscillating horizontal and vertical magnetic dipoles are calculated for loops placed above an n-layer earth. The formal solutions for the magnetic fields in air are presented in terms of three infinite integrals which may be evaluated numerically on a digital computer. A completely generalized computer program for that purpose has been included in this paper. The program has been used to make a detailed analysis of the polarization characteristics of the fields from airborne vertical and horizontal magnetic dipoles above a multi-layer earth. A number of theoretical curves show the variations of the tilt angle and ellipticity of the polarization ellipses over several models. Both tilt angle and ellipticity plots show good resolution but ellipticity plots have somewhat higher resolution. Hence both these parameters may be used in the interpretation of airborne electromagnetic mapping data.

## RÉSUMÉ

L'auteur calcule les champs électromagnétiques des dipôles oscillants horizontaux et verticaux dans le cas de boucles placées sur un nombre n de couches du globe terrestre. Les solutions régulières pour les champs magnétiques dans l'air sont présentées sous forme de trois intégrales infinies qu'on peut évaluer numériquement à l'aide d'un ordinateur. On trouvera dans cette étude un programme d'ordinateur complètement généralisé à cette fin. Ce programme a été utilisé afin d'effectuer une analyse détaillée des caractéristiques de la polarisation des champs à partir de dipôles magnétiques aériens verticaux et horizontaux au-dessus de plusieurs couches la. Plusieurs courbes théoriques montrent les variations de l'angle d'inclinaison et de l'ellipticité des ellipses de polarisation de plusieurs modèles. Les diagrammes d'angle d'inclinaison et d'ellipticité donnent de bonnes résolutions mais ceux d'ellipticité donnée des résolutions quelque peu plus élevées. De là, ces paramètres peuvent être utilisés dans l'interprétation de données fournis par les levés électromagnétiques aéroportés.



# ELECTROMAGNETIC FIELDS OF OSCILLATING MAGNETIC DIPOLES PLACED OVER A MULTILAYER CONDUCTING EARTH

---

## INTRODUCTION

Electromagnetic methods have long been used routinely in mining geophysics. Since large contrasts in electrical properties exist between most massive sulphide deposits and the surrounding host rocks, electromagnetic methods provide an excellent tool for the detection and delineation of such deposits. During the last few years, significant advances in instrumentation and in the theory of electromagnetic wave propagation in layered media have enhanced the prospect of applying these methods for routine sounding of stratified earth sections. This has application in the mapping of virgin areas as well as for specific purposes like the location and the delineation of the aquifers and water-tables for use in groundwater prospecting and in foundation engineering.

The most commonly used source of excitation in electromagnetic prospecting is the oscillating magnetic dipole, which is simply a small loop carrying low-frequency alternating current. The loop may be approximated to a dipole when the area of the loop is much smaller than the free-space wavelength and when the transmitter-receiver separation is at least 5 times the diameter of the loop. Various configurations of horizontal and vertical dipoles are used by different exploration companies for transmitting and receiving the fields. All these cases are described in detail by Parasnis (1970).

The problem of determining the electromagnetic fields of dipoles placed over a conductive earth has engaged the attention of many workers beginning with Sommerfeld's (1909, 1926) classic work. Later, Wait in a series of papers (1954, 1955, 1956) presented expressions for the mutual coupling ratios of ground and airborne dipoles placed above a homogeneous conducting earth. In a subsequent paper, he (Wait, 1958) extended his work to consider the case of a two-layer earth. The solutions, however, could not be expressed in terms of known functions and the numerical results could be obtained only by the numerical integration of a few infinite integrals on a digital computer. Frischknecht (1967) has presented extensive numerical results for the fields and mutual impedances on and above a two-layer medium for different configurations of dipoles. Recently, Dey and Ward (1970) and Ryu *et al.* (1970) have presented formal solutions for loops placed on an n-layer earth, taking the displacement current into consideration. However, for most geophysical exploration problems, displacement currents are almost always negligible.

It is known that in many areas, the earth section consists of more than two layers. In such cases, the technique of curve matching using the curves for a two-layer earth is inapplicable and a correct interpretation of the field data requires theoretical curves for a multi-layer earth. Although the formal solutions for an n-layer earth are available in literature (Wait, 1962, 1966; Dey and Ward, 1970), numerical results are somewhat scanty. It was

---

Original manuscript submitted: January 15, 1973

Final version approved for publication: April 26, 1973

Author's address: Geological Survey of Canada,  
601 Booth Street, Ottawa, Canada



therefore decided to present the complete method of determining the field components from dipoles placed over an n-layer earth. A computer program has been written for that purpose which is completely general except for the neglect of displacement currents in all the media (quasi-static case). Using the program, some results for the mutual coupling between a transmitter and a receiver in four standard coil arrangement systems used in airborne surveys have been obtained (Sinha, 1973) when flown over several three and four layer sections. It is realized, however, that since the possible number of independent parameters for an n-layer earth could be very large, any attempt to present master-charts for all the cases would be futile. The only practical solution in such a situation is to present the computer program for the calculation of the mutual coupling ratios so that anyone may obtain the desired theoretical curve for any set of data.

A very recent development in airborne electromagnetics is the prospect that multifrequency airborne systems will become available very shortly. The full potentials of these will be realized only if we are equipped with the means of interpreting the data quantitatively which would require a method of obtaining the theoretical response for any type of earth section. We have, therefore, presented the complete computer program for the determination of the polarization characteristics of the electromagnetic fields from airborne horizontal and vertical magnetic dipoles when flown over an n-layer earth. Three typical values of the ratio of the height of the system to their coil separation, characteristic of the helicopter and fixed-wing airborne systems have been considered over several three-layer models to illustrate the variation of the tilt angle and ellipticity values with the induction parameter from airborne horizontal and vertical magnetic dipoles. It is hoped that this study will be helpful in selecting the parameters to be chosen for the interpretation of the airborne E. M. survey data.

### MATHEMATICAL DEVELOPMENT

Let us suppose that an arbitrarily oriented magnetic dipole carrying a current  $I \exp(i\omega t)$  is placed at a height  $h$  over an n-layer earth as shown in Figure 1. The electrical constants of air are  $(\sigma_0, \mu, \epsilon_0)$  and that of the layers being taken as  $(\sigma_m, \mu, \epsilon_m)$ , where the subscript  $m$  varies from 1 to  $n$ . The permeabilities of all the layers are taken to be the same as that of vacuum and designed by  $\mu (4\pi \times 10^{-7} \text{h/m})$ . The thickness of the layers are denoted by  $d_m$  where  $m$  varies from 1 to  $(n-1)$ . The point of observation is taken to be any point  $P$  over the earth with coordinates  $(x, y, z)$  in cartesian system or  $(\rho, \phi, z)$  in cylindrical system. All the layers are assumed to be homogeneous and isotropic and all the interfaces have been assumed to be parallel to the air-earth boundary.

Since  $\text{div } \vec{E} = 0$ , the electromagnetic field components may be expressed in terms of a vector potential  $\vec{F}$  as:

$$\vec{E} = -\text{Curl } \vec{F} \quad (1)$$

$$i\omega\mu\vec{H} = \text{grad div } \vec{F} - \gamma^2\vec{F} \quad (2)$$

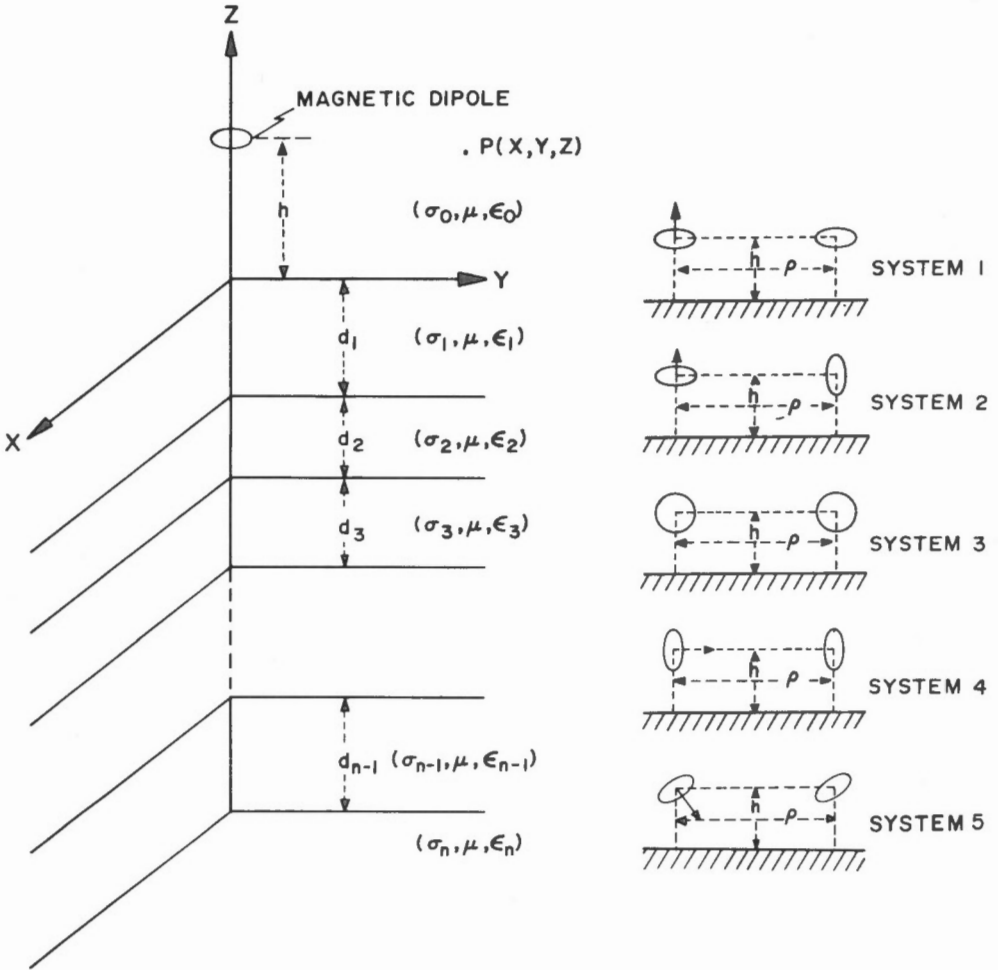


Figure 1. Magnetic dipole over an n-layer earth and the five coil arrangements considered in the text.

where  $\gamma = [i\omega\mu(\sigma + i\omega\epsilon)]^{1/2}$  is the propagation constant of the medium. In normal electromagnetic explorations, the frequency of the current is usually kept low and so the displacement currents are normally negligible compared to the conduction currents. Hence:

$$\gamma = (i\omega\mu\sigma)^{1/2} \quad \text{where } i = \sqrt{-1}. \quad (3)$$

The arbitrarily oriented dipole may be broken up into two component dipoles, one vertically, and the other horizontally directed. Considering the vertical dipole first (directed towards the positive Z-axis), from symmetry considerations it may be shown easily that the field components may be determined in this case from one component  $F_z$  only.

The secondary vector potential components in all the media would satisfy the Helmholtz equation:

$$(\nabla^2 - \gamma_m^2) F_{z_m}^s = 0 \quad (4)$$

where  $\gamma_m = (i\omega\mu\sigma_m)^{1/2}$  and  $m = 0, 1, 2, \dots, n$ .

The source vector potential  $F_{z_0}^p$  at  $P(\rho, \phi, z)$  in air is given by:

$$F_{z_0}^p = \frac{Me^{-\gamma_0 R}}{R} = \frac{IdA i\omega\mu}{4\pi} \int_0^\infty \frac{\lambda}{u_0} e^{-u_0|z-h|} J_0(\lambda\rho) d\lambda \quad (5)$$

$$\text{where } R = [\rho^2 + (z-h)^2]^{1/2}$$

$$\text{and } u_0 = (\lambda^2 + \gamma_0^2)^{1/2}$$

Here  $M$  and  $dA$  refer to the moment of the dipole and the area of the loop respectively,  $J_0(\lambda\rho)$  is a Bessel function of first kind and  $\lambda$  is the variable of integration.

From equation (4), the secondary vector potentials are given by:

$$F_{z_m}^s = \int_0^\infty A_m(\lambda) e^{\pm u_m z} J_0(\lambda\rho) d\lambda \quad (6)$$

where  $u_m = (\lambda^2 + \gamma_m^2)^{1/2}$ . We will thus have a series of equations specifying the vector potentials in all the media. The constants of integration  $A_m(\lambda)$  are evaluated by satisfying the boundary conditions at all the interfaces which specify the continuity of the tangential components of the electromagnetic fields at the interfaces.

If instead of the layered half-space, we have a homogeneous half-space with conductivity  $\sigma_1$ , the vector potential at any point  $P(\rho, \phi, z)$  in air may be written as:

$$F_{z_0}^p = \frac{IdA i\omega\mu}{4\pi} \int_0^\infty \left[ \frac{\lambda}{u_0} e^{-u_0|z-h|} + A_0(\lambda) e^{-u_0(z+h)} \right] J_0(\lambda\rho) d\lambda \quad (7)$$

$A_0(\lambda)$ , the constant of integration may be evaluated from the boundary conditions at  $z = 0$  as:

$$A_0(\lambda) = \frac{\lambda}{u_0} \left( \frac{u_0 - u_1}{u_0 + u_1} \right) \quad (8)$$

where the subscripts 0 and 1 refer to air and the earth respectively. Reverting to the case of an  $n$ -layer earth, it is clear that there will be  $(n + 1)$  equations for the vector potentials in  $(n + 1)$  media including air. Applying the boundary conditions to the bottom layer first and working progressively upward, we may obtain the new value of  $A_0(\lambda)$  in terms of the physical parameters of the layers as:

$$A_0(\lambda) = \frac{\lambda}{u_0} R_{TE}^v(\lambda) \quad (9)$$

where  $R_{TE}^v(\lambda)$  is the reflection coefficient for the TE component of the wave for the vertical dipole. From Wait (1962, 1966) we may write:

$$R_{TE}^v(\lambda) = \frac{N_0 - Y_1}{N_0 + Y_1} \quad (10)$$

where

$$Y_m = N_m \frac{Y_{m+1} + N_m \tanh(u_m d_m)}{N_m + Y_{m+1} \tanh(u_m d_m)} \quad (11)$$

$m = 1, 2, 3, \dots, (n-1)$

and  $Y_n = N_n$ ,  $N_m = \frac{u_m}{i\omega\mu}$  where  $m = 0, 1, 2, \dots, n$ . (12)

The  $Y_m$  values, in analogy with transmission line theory may be termed the surface admittances of the layers. Thus, we start by calculating  $Y_n$  for the bottom layer from equation (12) and then use its value in the mathematical algorithm of equation (11) to obtain the value of  $Y_{(n-1)}$  using the values of  $N_{(n-1)}$ ,  $u_{(n-1)}$  and  $d_{(n-1)}$ . This is continued until we obtain  $Y_1$  for the topmost layer.  $R_{TE}^v(\lambda)$  may easily be obtained from the values of  $Y_1$  and  $N_0$  obtained from equation (12).

Considering the horizontal magnetic dipole directed towards the Y-axis at the same location as the vertical dipole, it may be shown easily that in order to satisfy the boundary conditions at the interfaces, the secondary vector potential must have two components, one along the Y-axis and the other along the Z-axis.

If we now assume that we have a homogeneous half-space in place of the n-layer earth, the solution for the vector potential components at  $P(\rho, \phi, z)$  in air may be written as:

$$F_{y_0} = \frac{IdAiw\mu}{4\pi} \int_0^\infty \left[ \frac{\lambda}{u_0} e^{-u_0|z-h|} + B_0(\lambda) e^{-u_0(z+h)} \right] J_0(\lambda\rho) d\lambda \quad (13)$$

$$F_{z_0} = \frac{IdAiw\mu \cos\phi}{4\pi} \int_0^\infty C_0(\lambda) e^{-u_0(z+h)} J_1(\lambda\rho) d\lambda \quad (14)$$

$B_0(\lambda)$  and  $C_0(\lambda)$  may be evaluated from the boundary conditions as:

$$B_0(\lambda) = \frac{\lambda}{u_0} \left[ \frac{\gamma_1^2 u_0 - \gamma_0^2 u_1}{\gamma_1^2 u_0 + \gamma_0^2 u_1} \right] \quad (15)$$

$$C_0(\lambda) = \frac{2\lambda^2 (\gamma_0^2 - \gamma_1^2)}{(u_0 + u_1)(\gamma_1^2 u_0 + \gamma_0^2 u_1)} \quad (16)$$

Going back to our original problem of an n-layer earth, it is clear that we will then have  $2(n+1)$  equations for the vector potential components in the  $(n+1)$  media including air. Applying the boundary conditions to the bottom layer first and working progressively upward, the constants  $B_0(\lambda)$  and  $C_0(\lambda)$  may be evaluated as:

$$B_0(\lambda) = \frac{\lambda}{u_0} R_{TM}^h(\lambda) \quad (17)$$

$$C_o(\lambda) = -[R_{TM}^h(\lambda) + R_{TE}^h(\lambda)] \quad (18)$$

where  $R_{TM}^h(\lambda)$  and  $R_{TE}^h(\lambda)$  denote the reflection coefficients for the TM and the TE modes emitted by the horizontal magnetic dipole.  $R_{TM}^h(\lambda)$  may be written as (Wait, 1966):

$$R_{TM}^h(\lambda) = \frac{K_o - Z_1}{K_o + Z_1} \quad (19)$$

where

$$Z_m = K_m \cdot \frac{Z_{m+1} + K_m \tanh(u_m d_m)}{K_m + Z_{m+1} \tanh(u_m d_m)} \quad (20)$$

$$m = 1, 2, 3, \dots (n-1)$$

and

$$Z_n = K_n, \quad K_m = \frac{u_m}{(\sigma_m + i\omega \epsilon_m)} \approx \frac{u_m}{\sigma_m} \quad (21)$$

$$m = 0, 1, 2, \dots n$$

$R_{TE}^h(\lambda)$  has the same form as that given by equation (10).

The magnetic field components at any point above the earth may be obtained easily from equations (2), (7), (13) and (14). These equations are greatly simplified, however, by assuming  $\sigma_o$  to be infinitely small, i.e. we assume that the fields in air satisfy Laplace's equation instead of Helmholtz's equation. In such a case  $\gamma_o = 0$  and  $u_o = \lambda$ . Under this assumption, it is easy to show that the contribution of the TM mode to the magnetic field components in air cancel out (Dey and Ward, 1970), making the TE mode the only component giving rise to the magnetic fields in air. If the heights of the transmitter and receiver coils are  $h_1$  and  $h_2$  respectively, we can write down the expressions of the secondary fields as:

Vertical Magnetic Dipole:

$$H_{x,s} = \frac{IdA}{4\pi\delta^3} \cdot T_1(A, B, D_j, k_j) \left(\frac{x}{\rho}\right) \quad (22)$$

$$H_{y,s} = \frac{IdA}{4\pi\delta^3} \cdot T_1(A, B, D_j, k_j) \left(\frac{y}{\rho}\right) \quad (23)$$

$$H_{z,s} = \frac{IdA}{4\pi\delta^3} \cdot T_o(A, B, D_j, k_j) \quad (24)$$

Y-directed Horizontal Magnetic Dipole:

$$H_{x,s} = \frac{I dA}{4\pi\delta^3} \left[ \left( \frac{xy}{\rho^2} \right) \left\{ T_0(A, B, D_j, k_j) - \frac{2}{B} T_2(A, B, D_j, k_j) \right\} \right] \quad (25)$$

$$H_{y,s} = \frac{I dA}{4\pi\delta^3} \left[ \left( \frac{y^2}{\rho^2} \right) \left\{ T_0(A, B, D_j, k_j) + \frac{T_2(A, B, D_j, k_j)}{B} \left( \frac{\rho^2}{y^2} - 2 \right) \right\} \right] \quad (26)$$

$$H_{z,s} = - \frac{I dA}{4\pi\delta^3} \left[ \left( \frac{y}{\rho} \right) T_1(A, B, D_j, k_j) \right] \quad (27)$$

The response for the case of an inclined coil system may be obtained easily from the field values for the cases of horizontal and vertical magnetic dipoles given in equations (22) through (27).

Here:

$$T_0(A, B, D_j, k_j) = \int_0^\infty R_{TE}(g) g^2 e^{-gA} J_0(gB) dg \quad (28)$$

$$T_1(A, B, D_j, k_j) = \int_0^\infty R_{TE}(g) g^2 e^{-gA} J_1(gB) dg \quad (29)$$

$$T_2(A, B, D_j, k_j) = \int_0^\infty R_{TE}(g) g^2 e^{-gA} J_2(gB) dg \quad (30)$$

$$A = \frac{(h_1 + h_2)}{\delta}, \quad B = \frac{\rho}{\delta}, \quad D_j = \frac{2d_j}{\delta}, \quad k_j = \frac{\sigma_j}{\sigma_1}, \quad \delta = \left( \frac{2}{\omega\mu\sigma_1} \right)^{1/2}$$

where  $j = 1, 2, 3, \dots, n$ .

In airborne electromagnetic surveys, the parameter most commonly measured is the mutual impedance ratio rather than the fields. For two coplanar and coaxial loops separated by a distance  $\rho$  the mutual impedances  $Z_o$  between them when placed in free-space (Frischknecht, 1967) are:

$$Z_o = \frac{i\omega\mu dA_1 dA_2 N_1 N_2}{4\pi\rho^3} \quad \text{for a coplanar system} \quad (31)$$

and

$$Z_o = - \frac{i\omega\mu dA_1 dA_2 N_1 N_2}{2\pi\rho^3} \quad \text{for a coaxial system} \quad (32)$$

where  $dA_1$ ,  $dA_2$  and  $N_1$ ,  $N_2$  are the areas and the number of turns of the two loops. Thus the mutual coupling ratio  $Z/Z_o$  indicates the ratio of the mutual coupling between two loops in the presence of the earth and that in its absence.

The mutual coupling ratios for the five important coil systems shown in Figure 1 may be written down as:

System 1: Horizontal coplanar loops

$$Z/Z_0 = 1 - B^3 T_0 (A, B, D_j, \kappa_j) \quad (33)$$

System 2: Perpendicular loops

$$Z/Z_0 = -B^3 T_1 (A, B, D_j, \kappa_j) \quad (34)$$

System 3: Vertical coplanar loops

$$Z/Z_0 = 1 - B^2 T_2 (A, B, D_j, \kappa_j) \quad (35)$$

System 4: Vertical coaxial loops

$$Z/Z_0 = 1 + \frac{B^2}{2} \{ B T_0 (A, B, D_j, \kappa_j) - T_2 (A, B, D_j, \kappa_j) \} \quad (36)$$

It may be worthwhile to point out that in addition to the above standard systems, there exists another possibility for a null-coupled configuration. This system (used by Geonics EM-15 and Apex Systems) which employs two inclined loops (axes of the loops inclined at 54.7 degrees to the horizontal) is unique in one respect. Although the planes of the coils are parallel to each other (but not coplanar), it may be shown easily (A. Becker, pers. comm., 1972) that they are in minimum coupling position for any value of  $\rho$  (see Appendix I). This type of configuration has some advantages in the matter of mounting of the coils for airborne surveys, the mutual coupling ratio for which is given by:

System 5: Inclined parallel loops

$$Z/Z_0 = B^2 \left\{ \frac{T_2 (A, B, D_j, \kappa_j)}{3} - B T_0 (A, B, D_j, \kappa_j) \right\} \quad (37)$$

The infinite integrals  $T_0$ ,  $T_1$  and  $T_2$  are evaluated numerically by the Gaussian Quadrature technique. Since the integrals contain products involving Bessel functions, the products are oscillatory. Hence the integrals are divided into several segments bounded by the zeros of the Bessel functions and their contributions are evaluated separately. The total integrals are thus given by the algebraic sum of the contributions from all the segments (Abramowitz and Stegun, 1965).

TABLE I

Accuracy of the Gaussian method of integration with different abscissa and weight values (n)

Model Parameters:

$$\rho_1 = 10\Omega - m, \rho_2 = 1\Omega - m, \rho_3 = 10^3\Omega - m, d_1 = 10 \text{ m},$$

$$d_2 = 15 \text{ m and TR separation} = 25 \text{ m}.$$

All the computed values are for the first segment only.

A/B	B	n	-T <sub>0</sub>		-T <sub>1</sub>		-T <sub>2</sub>	
			Re	Im	Re	Im	Re	Im
4.0	.1	16	.479617	1.949552	.058347	.400845	.024108	.100551
4.0	.1	32	.478936	1.949066	.058246	.400767	.024228	.100390
4.0	.1	48	.478935	1.949066	.058245	.400766	.024228	.100389
4.0	.1	96	.478935	1.949066	.058245	.400766	.024228	.100389
4.0	.5	16	.092255	.038234	.024717	.014386	.024129	.010365
4.0	.5	32	.092255	.038234	.024717	.014386	.024129	.010365
4.0	.5	48	.092255	.038234	.024717	.014386	.024129	.010365
4.0	.5	96	.092255	.038234	.024717	.014386	.024129	.010365
6.0	.1	16	.315104	.992047	.030126	.151463	.015695	.050527
6.0	.1	32	.314492	.991480	.030037	.151372	.015834	.050383
6.0	.1	48	.314492	.991481	.030037	.151372	.015834	.050383
6.0	.1	96	.314492	.991481	.030037	.151372	.015834	.050383
6.0	.5	16	.038559	.011870	.007715	.003268	.009891	.003104
6.0	.5	32	.038559	.011870	.007715	.003268	.009891	.003104
6.0	.5	48	.038559	.011870	.007715	.003268	.009891	.003104
6.0	.5	96	.038559	.011870	.007715	.003268	.009891	.003104
10.0	.1	16	.166538	.373665	.011556	.038838	.008163	.018889
10.0	.1	32	.166092	.372966	.011492	.038729	.008333	.018785
10.0	.1	48	.166091	.372966	.011492	.038728	.008333	.018785
10.0	.1	96	.166091	.372966	.011492	.038728	.008333	.018785
10.0	.5	16	.010995	.002200	.001451	.000394	.002780	.000560
10.0	.5	32	.010995	.002200	.001451	.000394	.002780	.000560
10.0	.5	48	.010995	.002200	.001451	.000394	.002780	.000560
10.0	.5	96	.010995	.002200	.001451	.000394	.002780	.000560



Hence:

$$\int_0^{\infty} \Psi(A, B, D, k) J_m(gB) dg = \sum_{j=1}^{\infty} \frac{(x_j - x_{j-1})}{2} \sum_{p=1}^n w_p \{ \Psi_j(A, B, D, k) J_m(gB) \}_p + R_n \quad (38)$$

where  $x_j$  values are the zeros of  $J_m(gB)$ ,  $R_n$  is the remainder and

$\{ \Psi_j(A, B, D, k) J_m(gB) \}_p$  is that function evaluated at  $g_p$  given by

$$g_p = \frac{1}{2} \{ (x_j - x_{j-1}) x_p + (x_j + x_{j-1}) \} \quad (39)$$

where  $w_p$  and  $x_p$  are the weight factors and the abscissas for the Gaussian integration with  $n$  points. Tables for the weight factors and abscissas for different  $n$  values are available (Abramowitz and Stegun, 1965). However, considering a larger  $n$  means taking a narrower mesh, and hence the results should be more accurate in such cases. Although previous workers (Frischknecht, 1967; Dyck and Becker, 1971; Sinha, 1973) have considered 16 and 32 point formulas for the numerical integration of  $T_0$ ,  $T_1$  and  $T_2$ , a comparative study of the order of accuracy of the different cases with different  $n$  values is not available at present. Before proceeding further with our numerical computation, it was, therefore, decided to establish the accuracy of the different formulas with different  $n$  for a few trial cases. In order to save computer time, only the first segment of the integral up to the first zero of the Bessel function  $J_n$  was evaluated in each case. The results for one model are tabulated in Table 1 for two values of  $B$  and three values of  $A/B$ , typical for airborne surveys. Four sets with  $n = 16, 32, 48$  and  $96$  were computed. It is clear from the table that the 16 point formula is not adequate in most cases, while the 32 point formula gives results which may be erroneous only in the sixth place of decimal. Results with the 48 and 96 point formulas are identical up to six places of decimals. We therefore chose the 48 point formula for all our subsequent computations.

### DESCRIPTION OF THE PROGRAM

#### A. Main Program COMP:

The program COMP presented in Appendix II is the main program which was used to obtain the polarization characteristics (tilt and ellipticity) of the fields from airborne horizontal and vertical magnetic dipoles placed over an  $n$ -layer earth. The program accepts the values of  $B$  which are provided as DATA input  $X$  in card Nos. 41 and 42. Additional inputs are provided in card No. 53 (statement No. 42) containing information about the type of dipole source being considered (NN), number of layers (NUM), conductivity of the top layer ( $S_1$ ) and the conductivity ratios  $\sigma_m/\sigma_1$  (K(J)) starting from the bottom layer first. The next card contains the information about the station number (NO), the particular model number of any series (L), model series

number (LL), A/B value (AB) and the thickness of the layers (D(J)) beginning with the bottom layer value first, which is taken to be zero. The integer variable TEE which takes values of 0, 1 and 2 indicates the subscript of T being computed. The variables DEL and CS represent the skin depth,  $\delta$ , in the top layer and the factor  $\omega \mu \delta$  which are needed in the subroutine CALC which computes the real and imaginary parts of the complex integrals  $T_0$ ,  $T_1$  and  $T_2$ . The loop beginning in card No. 91 computes the results for all B values for the given values of inputs beginning in statement number 42. Once the complex integrals have been evaluated, their values are printed out (card No. 118 or 139 as the case may be). The tilt and ellipticity of the field can easily be obtained from these values. The final results for the tilt angle and ellipticity values at every value of B for a particular A/B value is given in output statements beginning in card No. 166. A sample output for two given sets of input data is shown at the end of the program in Appendix II.

#### B. Subroutine CALC:

This subroutine is called three times in the main program to obtain the real and the imaginary parts of the integrals  $T_0$ ,  $T_1$  and  $T_2$ . The subroutine has four types of DATA inputs for the parameters AW, W, X0 and X1. The parameters AW and W denote the abscissas (zeros of Legendre Polynomials) and the weight factors respectively. For a 48 point formula, the areas between successive zeros of the Bessel function are subdivided into 48 parts and hence AW and W have 48 values each. The parameters X0 and X1 denote the positions of the zeros of the Bessel function  $J_0(x)$  and  $J_1(x)$  respectively. Since 40 consecutive segments have been considered in this routine, X0 and X1 have 40 values each in the data input. At each value of AW for a segment,  $g_p$  and  $R_{TE}(g_p)$  are determined and hence the contribution to the integral. After all 48 AW values have been considered, the algebraic sum of all 48 contributions are computed which gives the contribution for one segment bounded by two successive zeros of the Bessel function. The contribution from the first segment is stored in the memory for use in subsequent tests for the truncation of the series. The test involves the calculation of the ratio of the absolute value of the contribution from a particular segment to that of the first one. When this ratio falls below a certain specified value ( $10^{-6}$  in our case) the computation stops and the computer adds up the algebraic sum of the contributions from all the segments. If this stage is not reached before 19 segments, Euler's transformation (Abramowitz and Stegun, 1965) is used to obtain the sum the series from the 20th to the 40th segment. This is added to the sum of the contributions from the first to the 19th segment to obtain the value of the integral.

#### C. Subroutine EULER and Functions JOX, J1X and GG:

When the series is slowly converging, i.e. when the ratio of the 40th segment to the first segment is greater than  $10^{-6}$ , the computer calls the subroutine EULER to sum up the series of values from the 20th to the 40th segment by applying Euler's transformation. This subroutine is called twice to determine the real and the imaginary parts of the sum indicated by EUSUR and EUSUI. The functions JOX and J1X are used to provide the values of the

Bessel functions of order 0 and 1 at any value of the argument. The function GG is used to determine the parameter  $g_p$  as defined earlier. The value of A actually determines how many segments are needed to evaluate an integral since a higher value of A in the factor  $\exp(-gA)$  would damp the oscillations quickly so that only a few segments will be needed to achieve the desired accuracy.

## RESULTS

### a. Polarization characteristics of the ellipse due to an airborne vertical dipole:

The mathematical formulation presented earlier may be applied in the interpretation of multifrequency airborne EM sounding data over a layered earth section. For the purpose of interpretation, two types of measurements may be made: (1) recording the different components (real and imaginary) of the electromagnetic field measured at suitable points in space, and (2) measuring the polarization characteristics of the ellipse of polarization. The first set of measurements have been studied in an earlier paper (Sinha, 1973). We propose to study the second set of measurements in this section.

The polarization characteristics consist of four parameters, the tilt angle, ellipticity and the amplitude and phase of the wave tilt. However, since the shape of the magnetic polarization ellipse is completely described by the first two parameters, we will confine our attention to them only. In addition, these two parameters also exhibit the most characteristic changes with the change of subsurface and system characteristics. The orientation of the magnetic polarization ellipse is indicated in Figure 2(a). The field components  $H_p$  along the Y-axis and  $H_z$  may be written as:

$$H_p = |H_y| e^{i\phi_p} \quad (40)$$

$$H_z = |H_z| e^{i\phi_z} \quad (41)$$

where  $\phi_p$  and  $\phi_z$  denote the phase values of the magnetic field components.

The tilt angle  $\alpha$ , defined as the inclination of the major axis from the horizontal is given by:

$$\alpha = \frac{1}{2} \tan^{-1} \left\{ \frac{2 |H_y| |H_z| \cos(\phi_z - \phi_p)}{|H_y|^2 - |H_z|^2} \right\} \quad (42)$$

The ellipticity is defined as the ratio of the minor to the major axis, i.e.  $|H_2| / |H_1|$ . It may be seen that:

$$\text{Ellipticity} = \frac{|H_2|}{|H_1|} = |\tan \alpha| \quad (43)$$

where

$$\chi = \frac{1}{2} \sin^{-1} \left\{ \frac{2 |H_y| |H_z| \sin(\phi_z - \phi_p)}{|H_y|^2 + |H_z|^2} \right\} \quad (44)$$

The measurement of the tilt angle and ellipticity has some operational advantages over the measurement of the field components. Since equations (42) and (44) involve only the ratios of two components, no knowledge about the dipole moment is needed. Furthermore, in a ratio measuring technique, the measuring system need not be calibrated precisely for each component. Instrument drifts are also relatively unimportant since they tend to affect both components equally. As the primary field is 'bucked out' in most airborne systems, we have considered only the secondary fields of  $H_\rho$  and  $H_z$  for the determination of the polarization characteristics over a layered earth.

Tilt angle and ellipticity have been computed over 8 different 3-layer models. The first four models, designated as belonging to series 1 have the top layer resistivity  $\rho_1 = 10 \Omega - m$  and have been designated by symbols A, B, C and D. Similarly, the last four models have the top layer resistivity  $\rho_1 = 100 \Omega - m$  and have been designated as belonging to series 2, the individual models bearing symbol names A, B, ... D as before. The thicknesses of the layers are  $d_1 = 10$  m and  $d_2 = 15$  m for all the models and the separation between the transmitter and the receiver has been taken to be 25 metres. The parameters of the models have been shown in Fig. 2(b). The variations of the tilt angle and ellipticity with B (plotted on log-scale) for the four models of series 1 have been shown in Figures 3 through 8. The computations have been made for three A/B values, namely, A/B = 4.0, 6.0 and 10.0 which cover the range of values typical of fixed-wing and helicopter-borne systems. In all cases, the tilt angles show a monotonous decrease with the increase of B whereas the ellipticity values reach a maximum for certain values of B and then decrease toward zero. Sometimes, more than one peak may be present (e.g., Model A) before the ellipticity falls off to zero.

It is interesting to note that for series 1, the largest anomaly in tilt angle occurs in model B for the range of the parameter B considered here. This is true for all A/B values. For ellipticity, however, model C exhibits the largest anomaly followed by that in model D over the range of B considered. It may be noted that the ellipticity scale has been multiplied by 0.1 in each case, e.g., for B = 0.1 and A/B = 4.0, the value is 0.03484 for model A.

Figures 9 through 14 illustrate the variation of the tilt angle and ellipticity with B for three values of A/B for the four models belonging to series 2. The largest anomaly in tilt angle is obtained in model D for all three values of A/B considered here. The response for models B and C are very close, which differ only in the value of the bottom layer resistivity. Ellipticity variations are somewhat complicated particularly for model A which shows two or more peaks. However, as in case of tilt angle, model D (homogeneous case) produces the largest anomaly in ellipticity also. The resolution between the models B and C is however much better in the ellipticity plots.

#### b. Polarization characteristics of a horizontal magnetic dipole field:

The polarization characteristics of the ellipse of polarization due to an airborne horizontal magnetic dipole has been studied in a similar way. As

before, only tilt angle and ellipticity variations have been considered for the eight 3-layer models belonging to series 1 and 2 for the three A/B values. Figures 15 through 17 show the variations of the tilt angle with B for the four models of series 1.

The most obvious thing to note in those diagrams is that the tilt angles are negatives in this case and hence the general orientation of the ellipse is different. The absolute tilt angle values also tend to increase with B in these figures. This trend is not maintained however at larger values of B when the absolute value of the tilt angles begin to decrease and become very small at very high values of B. Such high values of B are, however, unrealistically large for existing airborne systems and hence these results have not been plotted. The magnitudes of the tilt angle anomalies are about twice as large in this case than in the case of a vertical dipole. The remarkable similarity between the shapes of the tilt angle and ellipticity plots for any model for both horizontal and vertical dipoles should be noted. However, the magnitudes of the anomalies are quite different in the two cases.

The largest anomalies in the tilt angle are obtained for the model B for all three values of A/B for the range of B values considered here. It should be noted, however, that when A/B ratio is high, the tilt angle variations for all the models are quite flat and hence, tilt angle measurements may be of doubtful use in such cases.

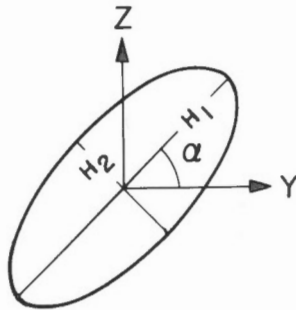
The variations of the ellipticity with B for models of series 1 are shown in Figures 18 through 20. Here, the largest anomaly is recorded for model C followed by that in model D. In general, the ellipticity anomalies in this case are about twice as large as the corresponding cases in case of a vertical dipole. The resolutions in the ellipticity plots are quite good indicating thereby that these may be used in the interpretation of airborne EM data even for large A/B ratios.

Similar curves have been plotted for the models of series 2 in Figures 21 through 26. As in the case of vertical dipoles, both tilt and ellipticity plots indicate that model D (homogeneous case) produces the largest anomalies in both. However, ellipticity plots show much greater resolution than the tilt angle plots. This indicates that ellipticity is probably a better diagnostic tool for airborne EM interpretation than the tilt angle.

### CONCLUDING REMARKS

For the interpretation of electromagnetic sounding data over a layered earth, we need to know the theoretical response of various layered models. It is clear however that for a multi-layer earth, the number of possible parameters could be large and so any attempt to present master-charts for all the cases would be futile. Therefore, a computer program for determining the polarization characteristics of the electromagnetic fields of oscillating magnetic dipoles placed over an n-layer earth has been presented in Appendix II so that anyone may obtain the theoretical response for a given model for comparison with the experimental data. The program is quite general in that the number of layers and their electrical parameters can be arbitrary. The only assumption made in this analysis is that the fields are quasi-static in nature, i.e. the displacement currents are negligible in comparison to the conduction currents. The solution mainly involves the determination of the reflection coefficient  $R_{TE}$  for the earth section with the help of an algorithm and using that value to integrate numerically three infinite integrals on a digital computer.

## POLARIZATION ELLIPSE



TILT ANGLE =  $\alpha$

$$\text{ELLIPTICITY} = \frac{|H_2|}{|H_1|}$$

Figure 2(a). Tilt angle and ellipticity for an elliptically polarized field.

## PARAMETERS OF THE MODELS CONSIDERED

$d_1 = 10\text{ m}, d_2 = 15\text{ m}, \text{TR SEPARATION} = 25\text{ m}$

<u>MODEL</u>	<u>SERIES 1</u>				<u>MODEL</u>	<u>SERIES 2</u>			
	<u>A</u>	<u>B</u>	<u>C</u>	<u>D</u>		<u>A</u>	<u>B</u>	<u>C</u>	<u>D</u>
$\rho_1(\Omega\text{-m})$	$10^1$	$10^1$	$10^1$	$10^1$	$\rho_1(\Omega\text{-m})$	$10^2$	$10^2$	$10^2$	$10^2$
$\rho_2(\Omega\text{-m})$	$10^2$	$10^2$	$10^2$	$10^3$	$\rho_2(\Omega\text{-m})$	$10^1$	$10^1$	$10^1$	$10^2$
$\rho_3(\Omega\text{-m})$	$10^0$	$10^1$	$10^3$	$10^2$	$\rho_3(\Omega\text{-m})$	$10^0$	$10^2$	$10^3$	$10^2$

Figure 2(b). Parameters of the models considered in the text.

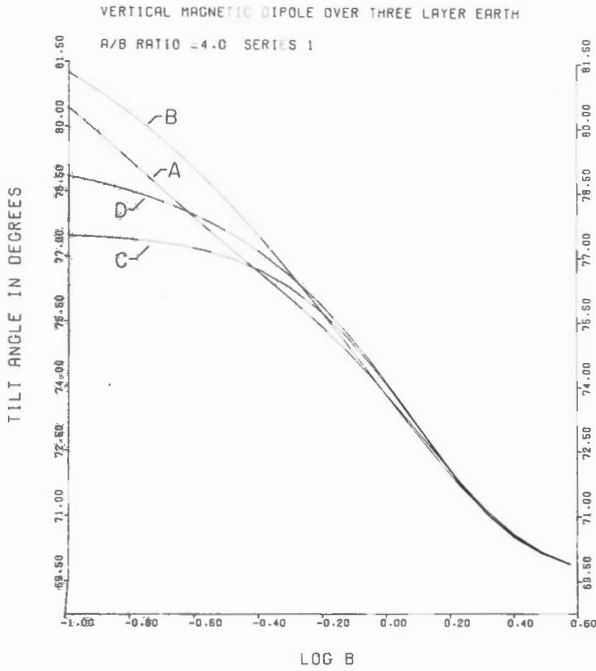


Figure 3.

Tilt angle versus B for the four models of series 1 for a vertical magnetic dipole with  $A/B = 4.0$ .

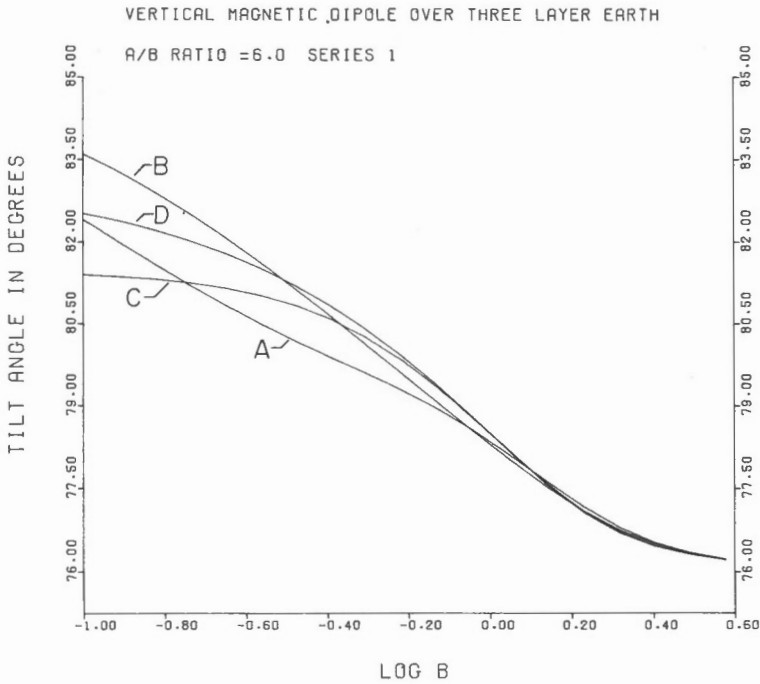


Figure 4. Tilt angle versus B for the four models of series 1 for a vertical magnetic dipole with  $A/B = 6.0$ .

VERTICAL MAGNETIC DIPOLE OVER THREE LAYER EARTH

A/B RATIO = 10.0 SERIES 1

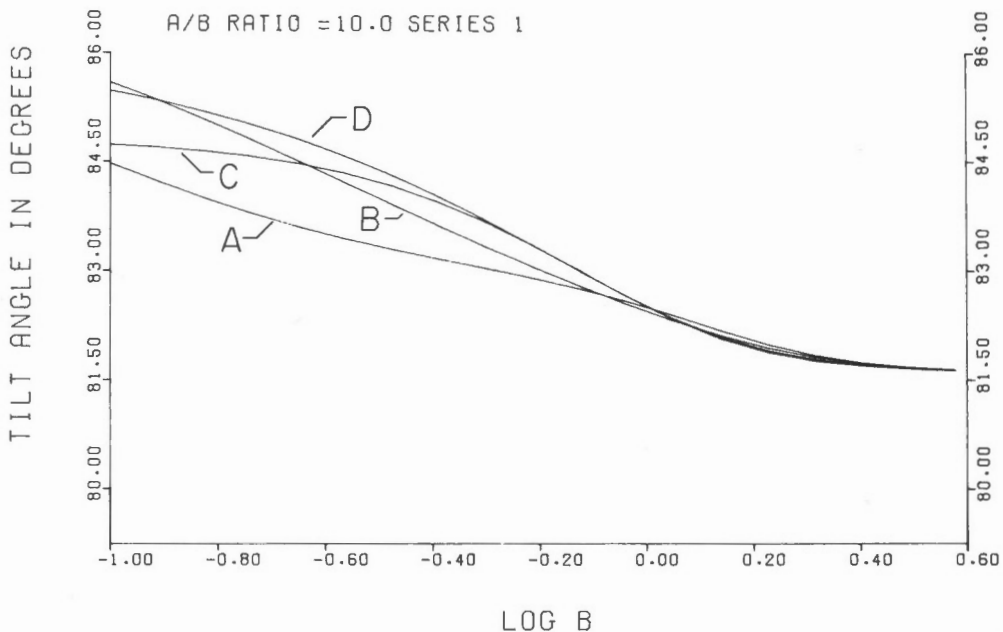


Figure 5. Tilt angle versus B for the four models of series 1 for a vertical magnetic dipole with A/B = 10.0.

VERTICAL MAGNETIC DIPOLE OVER THREE LAYER EARTH

A/B RATIO = 4.0 SERIES 1

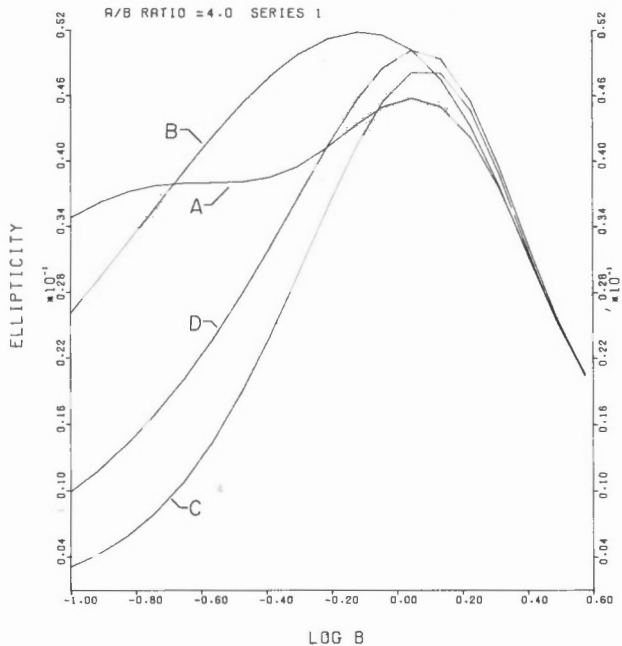


Figure 6.

Ellipticity versus B for the four models of series 1 for a vertical magnetic dipole with A/B = 4.0.



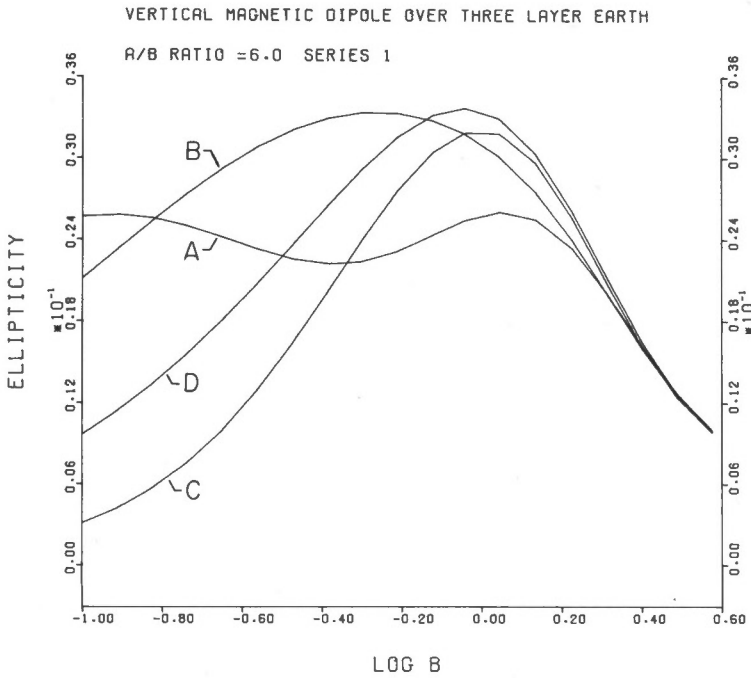


Figure 7. Ellipticity versus B for the four models of series 1 for a vertical magnetic dipole with A/B = 6.0.

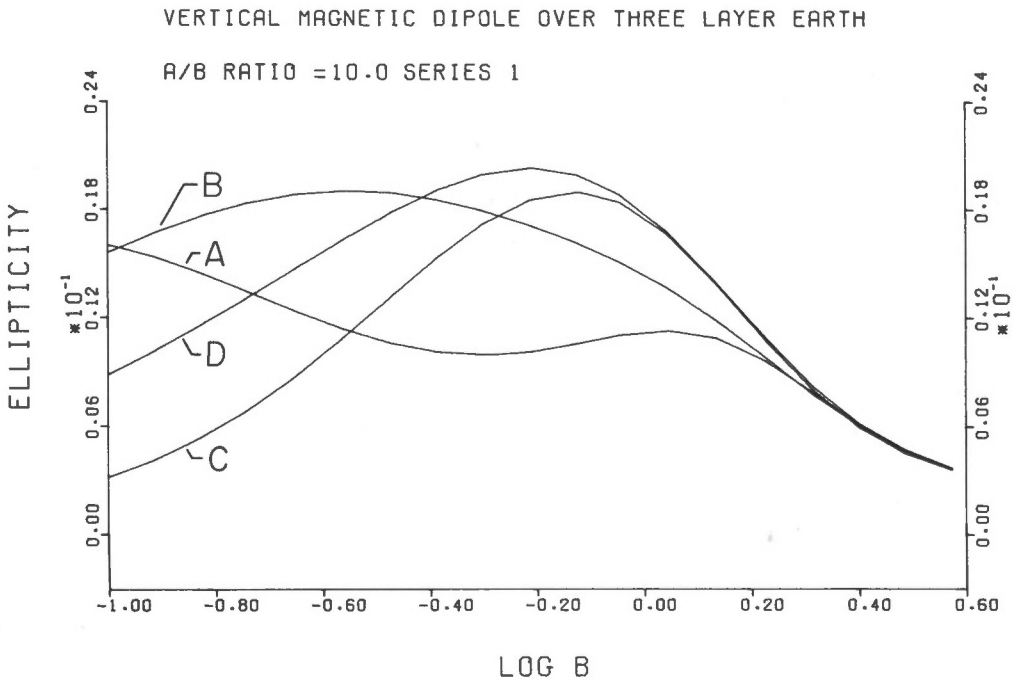


Figure 8. Ellipticity versus B for the four models of series 1 for a vertical magnetic dipole with A/B = 10.0.

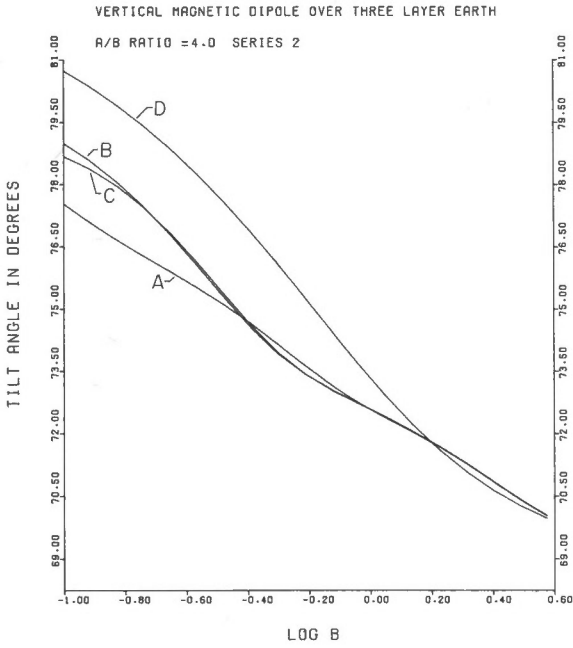


Figure 9.

Plot of the tilt angle versus B for the four models of series 2 for a vertical magnetic dipole with  $A/B = 4.0$

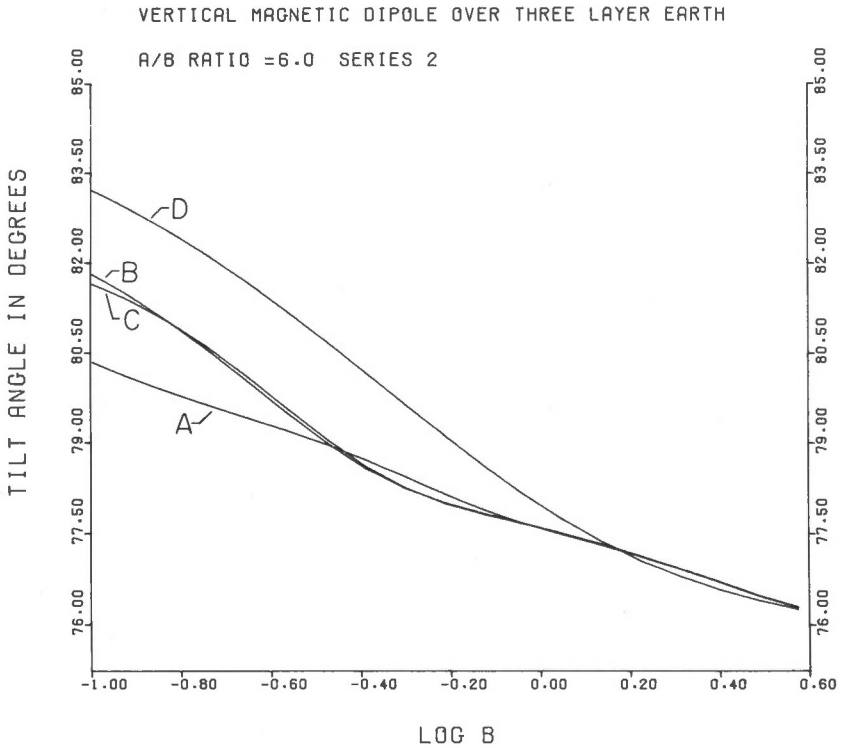


Figure 10. Plot of the tilt angle versus B for the four models of series 2 for a vertical magnetic dipole with  $A/B = 6.0$ .

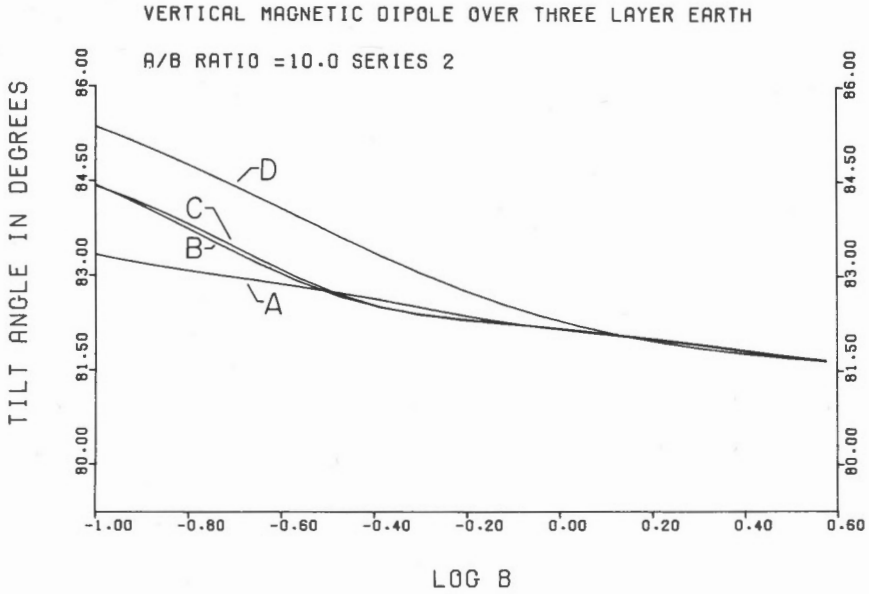


Figure 11. Plot of the tilt angle versus B for the four models of series 2 for a vertical magnetic dipole with A/B = 10.0.

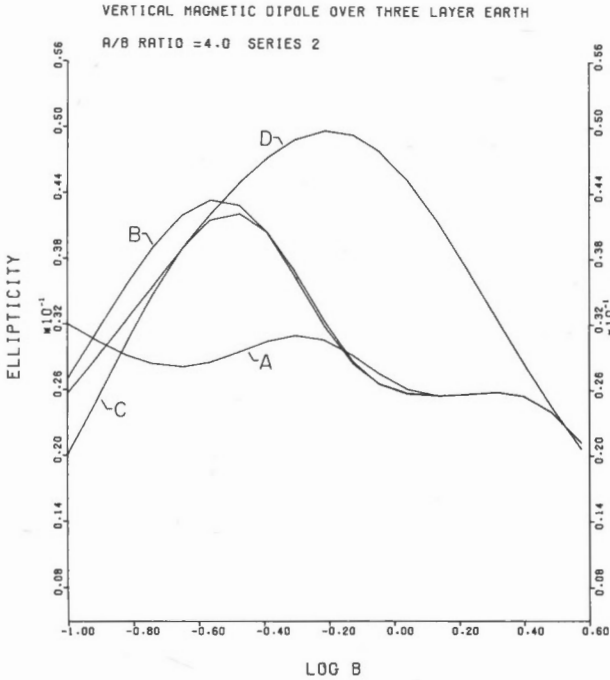


Figure 12. Plot of the ellipticity versus B for the four models of series 2 for a vertical magnetic dipole with A/B = 4.0.

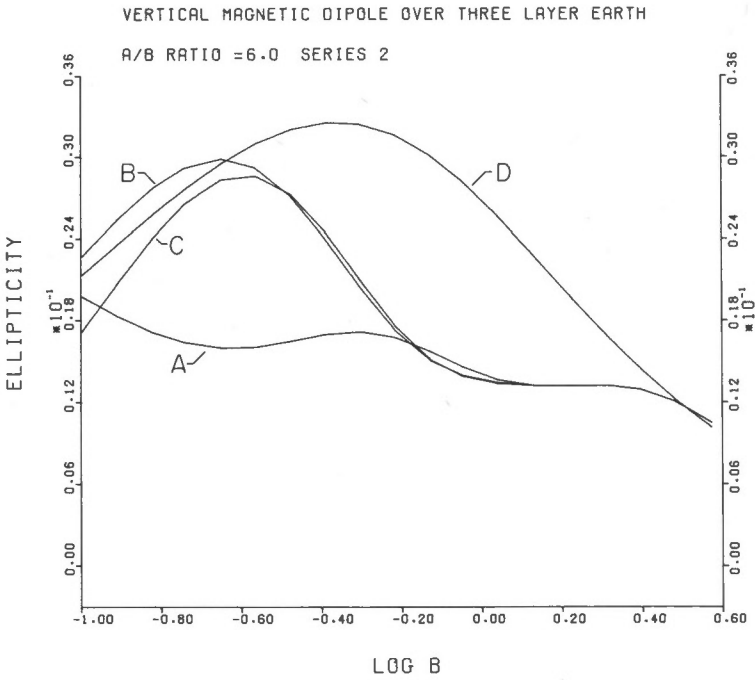


Figure 13. Plot of the ellipticity versus B for the four models of series 2 for a vertical magnetic dipole with  $A/B = 6.0$ .

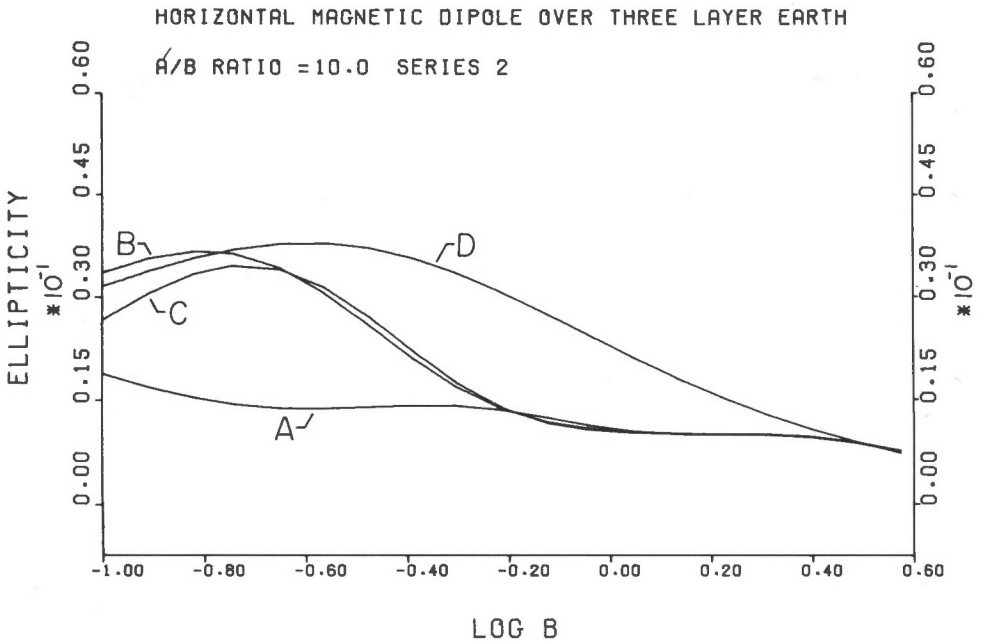


Figure 14. Plot of the ellipticity versus B for the four models of series 2 for a vertical magnetic dipole with  $A/B = 10.0$ .

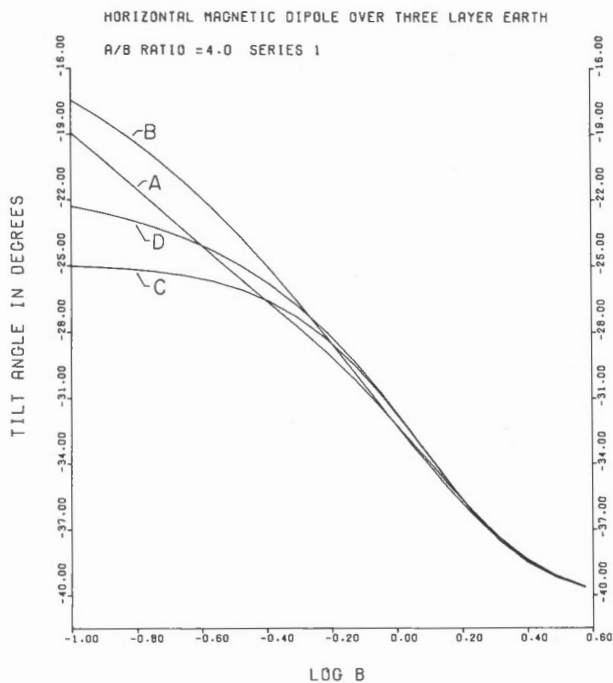


Figure 15. Tilt angle versus B for the four models of series 1 for a horizontal magnetic dipole with  $A/B = 4.0$ .

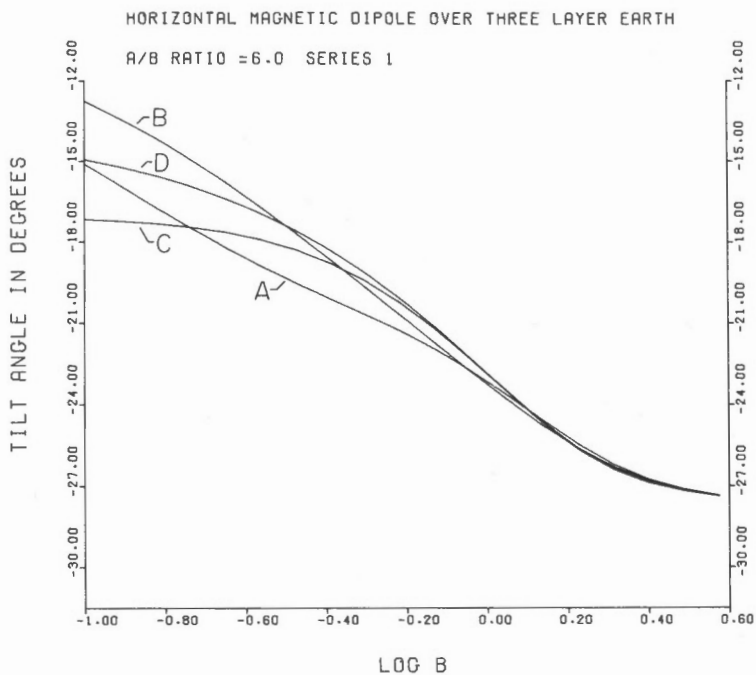


Figure 16. Tilt angle versus B for the four models of series 1 for a horizontal magnetic dipole with  $A/B = 6.0$ .

HORIZONTAL MAGNETIC DIPOLE OVER THREE LAYER EARTH

A/B RATIO = 10.0 SERIES 1

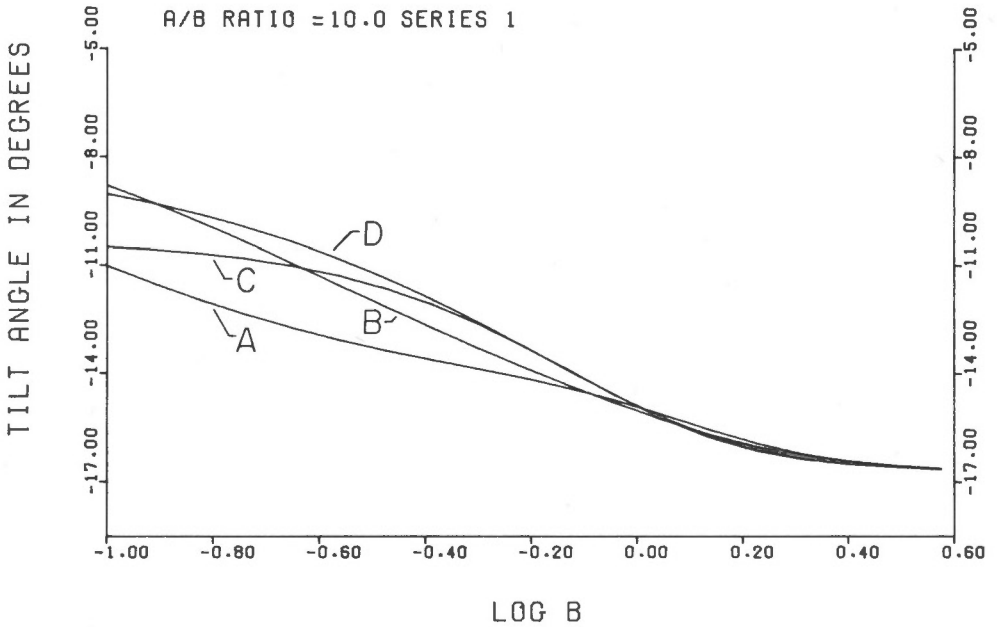


Figure 17. Tilt angle versus B for the four models of series 1 for a horizontal magnetic dipole with A/B = 10.0.

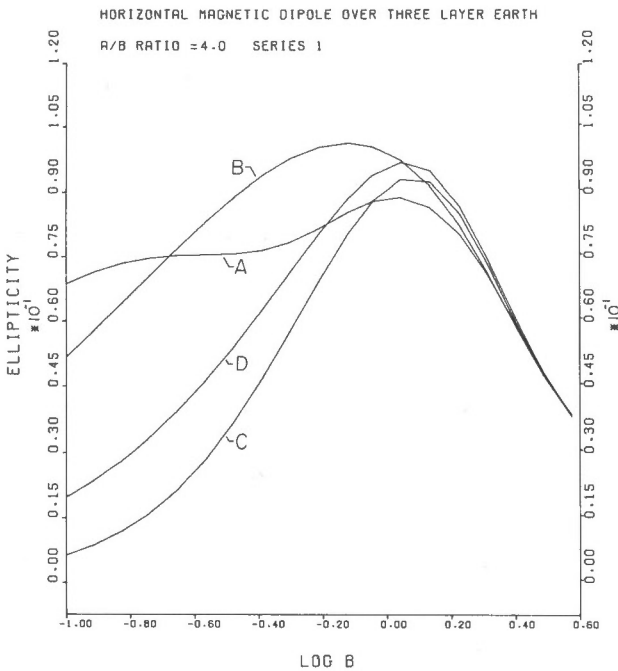


Figure 18. Ellipticity versus B for the four models of series 1 for a horizontal magnetic dipole with A/B = 4.0.

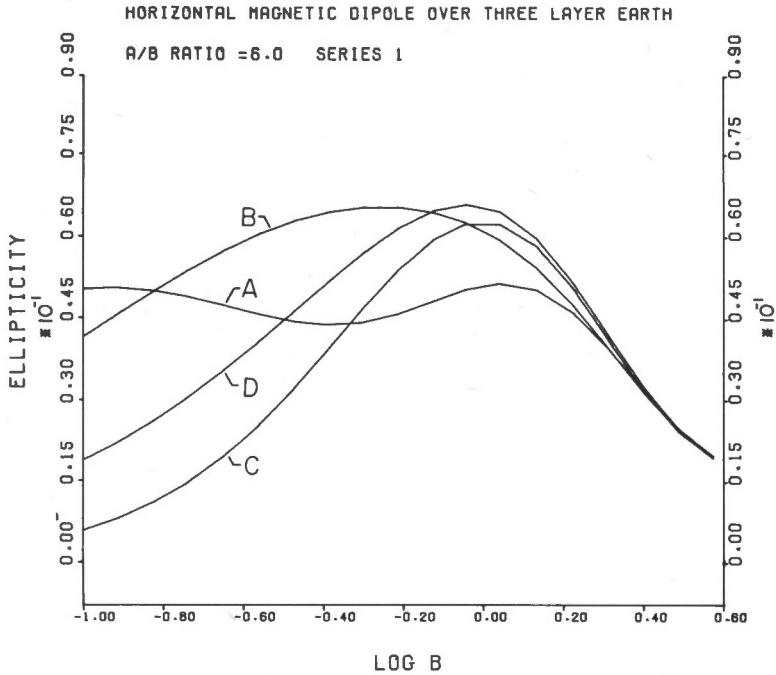


Figure 19. Ellipticity versus B for the four models of series 1 for a horizontal magnetic dipole with  $A/B = 6.0$ .

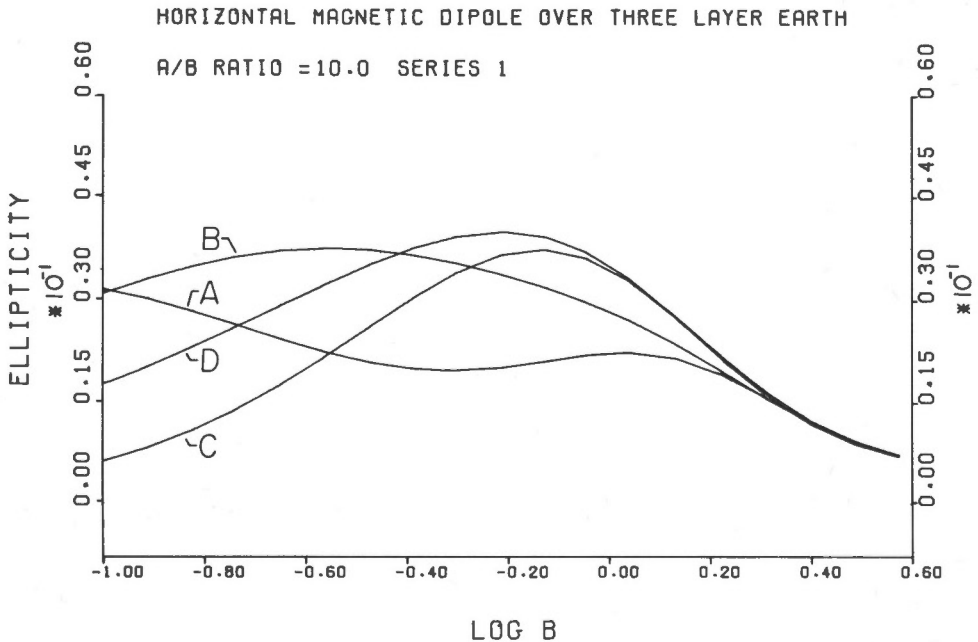


Figure 20. Ellipticity versus B for the four models of series 1 for a horizontal magnetic dipole with  $A/B = 10.0$ .

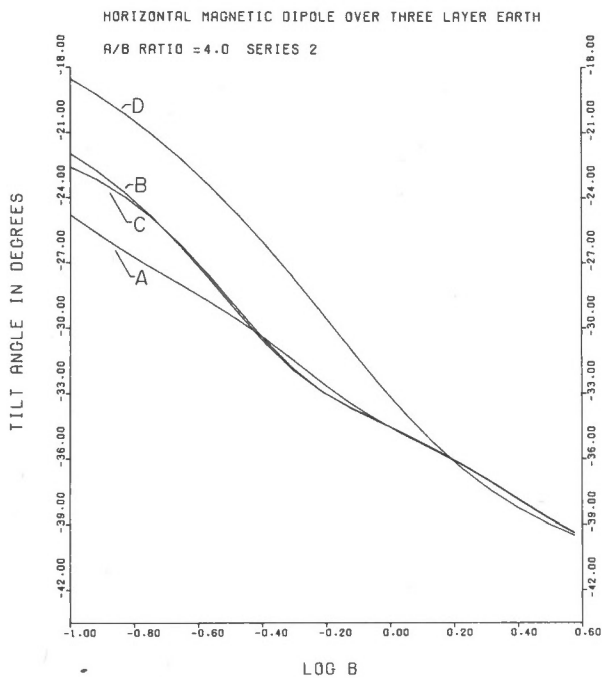


Figure 21.

Plot of the tilt angle versus B for the four models of series 2 for a horizontal magnetic dipole with  $A/B = 4.0$ .

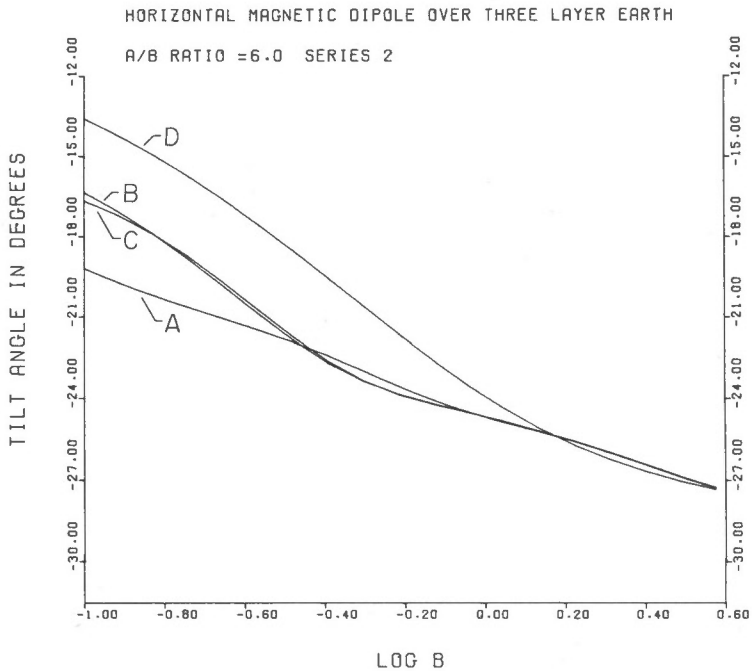


Figure 22. Plot of the tilt angle versus B for the four models of series 2 for a horizontal magnetic dipole with  $A/B = 6.0$ .



HORIZONTAL MAGNETIC DIPOLE OVER THREE LAYER EARTH

A/B RATIO = 10.0 SERIES 2

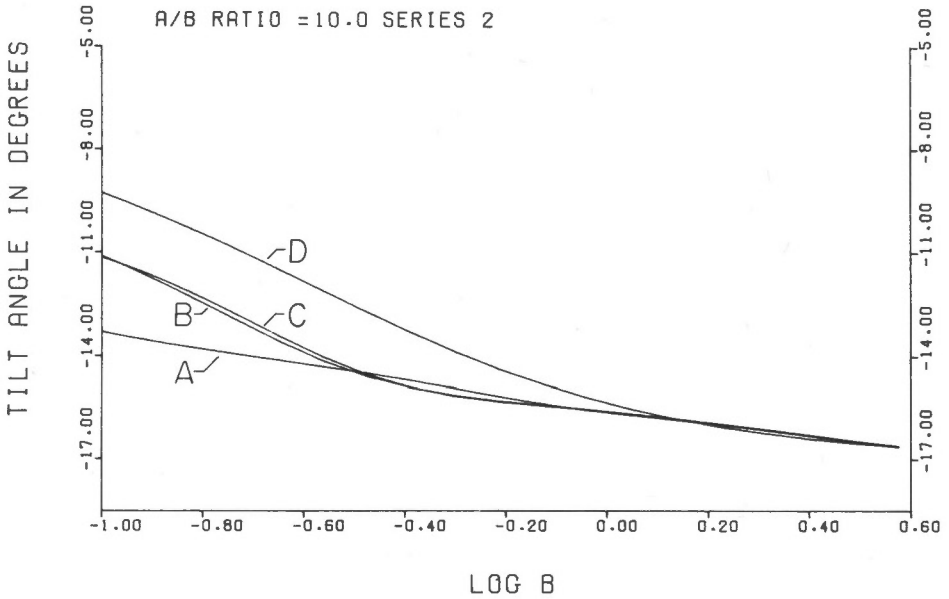


Figure 23. Plot of the tilt angle versus B for the four models of series 2 for a horizontal magnetic dipole with A/B = 10.0.

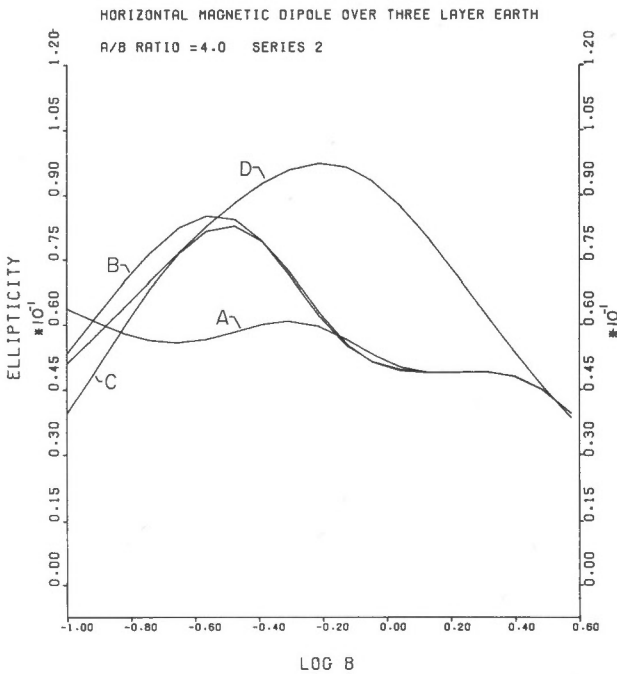


Figure 24. Plot of the ellipticity versus B for the four models of series 2 for a horizontal magnetic dipole with A/B = 4.0.

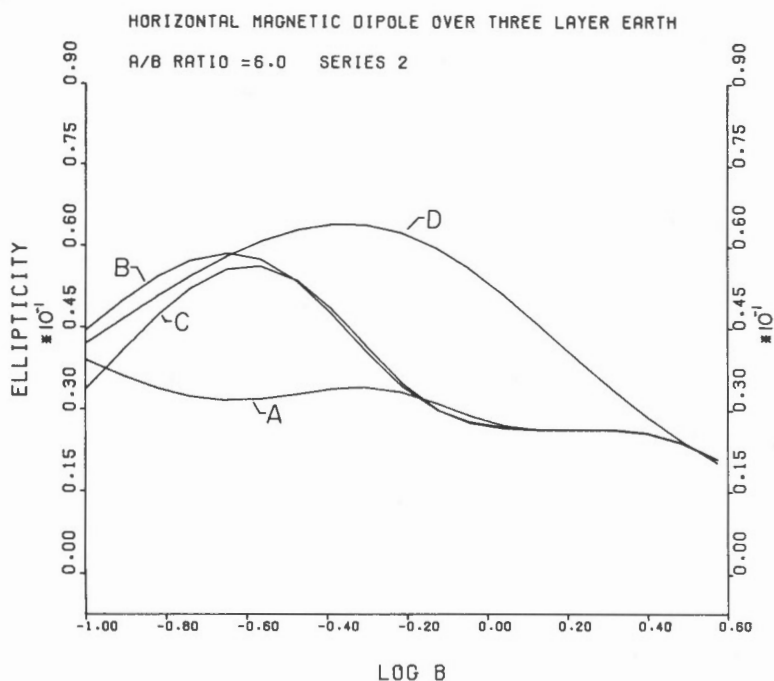


Figure 25. Plot of the ellipticity versus B for the four models of series 2 for a horizontal magnetic dipole with  $A/B = 6.0$ .

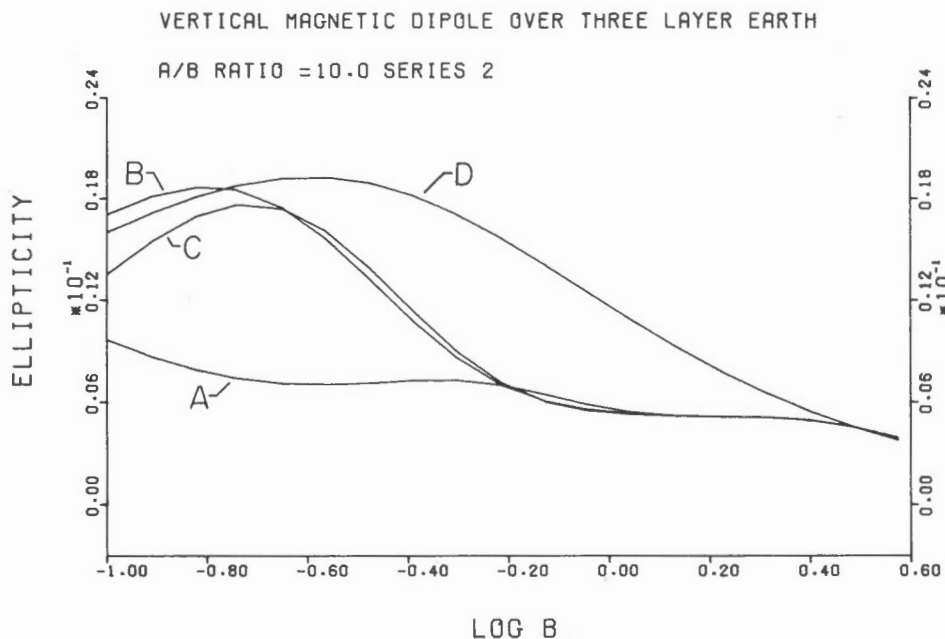


Figure 26. Plot of the ellipticity versus B for the four models of series 2 for a horizontal magnetic dipole with  $A/B = 10.0$ .

The program has been used to study the variations of the tilt angle and the ellipticity of the field ellipse for several models when excited by airborne vertical and horizontal magnetic dipoles. Both parameters show good resolution but the resolution is much better for the ellipticity. It is interesting to note that the shapes of the tilt and ellipticity plots for any model are remarkably similar for both horizontal and vertical dipoles. However, the magnitude of the anomaly for the horizontal dipole is about twice as large as that for the case of the vertical dipole, not to mention the different orientation of their tilt angles. The results indicate that the tilt and ellipticity of the magnetic polarization ellipse may be employed as parameters in the interpretation of multi-frequency airborne electromagnetic data.

#### ACKNOWLEDGMENTS

A part of the subroutine CALC used for the numerical evaluation of the integrals has been borrowed from the two-layer program of Dr. F.C. Frischknecht of the U.S. Geological Survey. We sincerely thank him for this. We are thankful to Dr. A. Becker for his critical reading of the manuscript.

#### REFERENCES

- Abramowitz, M., and Stegun, I. A.  
1965: Handbook of mathematical functions; Dover Publications Inc., New York.
- Dey, A., and Ward, S.H.  
1970: Inductive sounding of a layered earth with a horizontal magnetic dipole; Geophysics, v. 35, no. 5, p. 660-703.
- Dyck, A.V., and Becker, A.  
1971: Secondary fields of a vertical magnetic dipole above a thin horizontal layer of conductive overburden; Geol. Surv. Can., Paper 71-18, 25 p.
- Frischknecht, F.C.  
1967: Fields about an oscillating magnetic dipole over a two-layer earth and applications to ground and airborne electromagnetic surveys; Colo. Sch. Mines, Quart., v. 62, no. 1, 326 p.
- Parasnis, D.S.  
1970: An elegant universal nomenclature for electromagnetic moving source - receiver dipole configurations; Geophys. Prospect., v. 16, no. 1, p. 88-102.
- Ryu, J., Morrison, H.F., and Ward, S.H.  
1970: Electromagnetic fields about a loop source of current; Geophysics, v. 35, no. 5, p. 862-896.

Sinha, A.K.

- 1973: Comparison of airborne E.M. coil systems placed over a multi-layer conducting earth; *Geophysics*, v. 38, no. 5.

Sommerfeld, A.

- 1909: Über die Ausbreitung der Wellen in der drahtlosen telegraphie; *Ann. der Physik*, v. 28, p. 665-737.
- 1926: Über die Ausbreitung der Wellen in der drahtlosen telegraphie; *Ann. der Physik*, v. 81, p. 1135-1153.

Wait, J.R.

- 1954: Mutual coupling of loops lying on the ground; *Geophysics*, v. 19, no. 2, p. 290-296.
- 1955: Mutual electromagnetic coupling of loops over a homogeneous ground, *Geophysics*, v. 20, no. 3, p. 630-637.
- 1956: Mutual electromagnetic coupling of loops over a homogeneous ground - an additional note; *Geophysics*, v. 21, no. 2, p. 479-484.
- 1958: Induction by an oscillating magnetic dipole over a two-layer ground; *Appl. Sci. Res., Sec. B*, v. 7, p. 73-80.
- 1962: *Electromagnetic waves in stratified media*; Pergamon Press, Oxford.
- 1966: Fields of a horizontal dipole over a stratified anisotropic half-space; *Inst. Elec. Electron. Eng. Trans. on Ant. Prop.*, v. AP-14, no. 11, p. 790-792.

APPENDIX I

PROOF OF MINIMUM COUPLING BETWEEN THE COILS IN SYSTEM 5

Let us assume that the axis of the inclined transmitter coil makes an angle  $\theta$  with the horizontal. Resolving the moment  $M$  of the dipole into two components  $M_y$  and  $M_z$  along the horizontal and the vertical directions respectively, we have:

$$M_y = M \cos \theta \quad \text{and} \quad M_z = M \sin \theta$$

If the receiver coil is placed at a distance  $\rho$  from the transmitter along the  $y$ -axis and if the inclination of the axis of the receiver coil from the horizontal be denoted by  $\phi$ , then the field components at the receiver are:

$$H_y = \frac{2M_y}{\rho^3} \quad , \quad H_z = \frac{2M_z}{\rho^3}$$

The field recorded by the receiver is:

$$\begin{aligned} H &= H_y \cos \phi - H_z \sin \phi \\ &= \frac{M \cos \theta \cos \phi}{\rho^3} [2 - \tan \theta \tan \phi] \end{aligned}$$

Hence the field at the receiver will vanish whenever the relation  $\tan \theta \cdot \tan \phi = 2$  is satisfied. A particularly useful configuration of coils results when they are parallel to each other, i.e.  $\theta = \phi$ . It is easy to show from the above equation that when  $\theta = \phi = 54.7$  degrees, the coils are null-coupled to each other but maximally coupled to the secondary fields from a layered earth (see text). One advantage of System 5 is that small relative rotation of the coils produces about 40 per cent less noise in this system compared to the other null-coupled system (System 2) considered in this paper. This type of parallel-coil, rigidly held configuration is highly suitable for use in a helicopter-towed boom.

APPENDIX II

COMPUTER PROGRAM FOR DETERMINING THE POLARIZATION  
CHARACTERISTICS OF THE E.M. FIELDS\* DUE TO AIRBORNE DIPOLES  
-----

\*Copies of the program in deck form is available from the Geological Survey of Canada, on a user's cost basis. Arrangements should be made through the office of the Chief, Resource Geophysics and Geochemistry Division.

```

PROGRAM          COMP          TRACE          CDC 6400 FTN V3.0-P206 OPT=0 17/04/73 12.20.50.
*****
C PROGRAM COMP (INPUT,OUTPUT,TAPE5=INPUT,TAPE6=OUTPUT)
C *****
C PROGRAM TO COMPUTE THE TLI AND FLIPLICITY VALUES FOR AIRBORNE
C HORIZONTAL AND VERTICAL MAGNETIC DIPOLES OVER A LAYERED EARTH.
5 C TAPES = INPUT MEANS THAT THE VALUES ARE TO BE FOUND ON THE CARD READER.
C TAPES = OUTPUT MEANS THAT THE VALUES SPECIFIED ARE TO BE PLACED
C ON THE LINE PRINTER.
C *****
C DEFINITIONS OF THE DIFFERENT PARAMETERS USED
10 C NN= INTEGER VALUE (1 OR 2) INDICATING WHAT TYPE OF DIPOLE SOURCE
C IS BEING CONSIDERED.
C NUM = NUMBER OF LAYERS OF THE EARTH SECTION
C S1 = THE CONDUCTIVITY OF THE TOPMOST LAYER
C K(M) = VALUES OF SIGMA(M)/S1, WHERE SIGMA(M) IS THE CONDUCTIVITY
15 C OF THE MTH LAYER. THE VALUES OF K(M) START FROM THE BOTTOMMOST
C LAYER(LARGEST M) AND GO UPWARDS TO THE VALUE OF K(1) = 1.
C NO = THE STATION NUMBER
C L = INTEGER VALUE INDICATING WHICH PARTICULAR MODEL OF THE TWO
C MODEL SERIES IS BEING CONSIDERED.
20 C LL= MODEL SERIES NUMBER(1 OR 2).
C AR= THE VALUE OF A/R BEING CONSIDERED.
C D(M) = THICKNESS OF THE LAYERS STARTING WITH THE BOTTOMMOST VALUE
C FIRST, THAT IS D(M) = 0., AND THEN GRADUALLY MOVING UPWARDS.
C DEL = SKIN DEPTH IN METRES IN THE TOP LAYER
C THIS COMPUTATION ASSUMES THE TRANSMITTER-RECEIVER SEPARATION TO
25 C BE EQUAL TO 25.0 METERS.
C *****
C X VALUES INDICATE THE VALUES OF THE INDUCTION PARAMETER B
C DIMENSION THE REAL VALUE ARRAYS X AND D
30 C *****
C DIMENSION RE(30),OD(30),REE(30),ODD(30),RA1(30),AIM1(30),RA2(30)
C DIMENSION AIM2(30),Q1(30),R2(30),PH1(30),PH2(30),ALF(30),BLF(30)
C DIMENSION CLF(30),PETP(30),ELL(30)
C DIMENSION X(30),REAL(30),QUAD(30)
C REAL K(R),D(R)
C INTEGER TEE
C PIF= 3.141592653

```

```

C*****
C PRESENTATION OF X APPAYS AS DATA INPUT
C*****
40 DATA X/1.122,15.18,223.272,335.408,495.61,75.9,1.1,
DATA W/19/
C*****
45 C WRITE THE ORIGINAL TITLE ON THE LINE PRINTER.
C*****
WRITE (6,I89)
189 FORMAT (1H,* RESULTS FOR A NEW SFT OF DATA **/)
C*****
C READ THE DATA VALUES REQUIRED FOR SUBSEQUENT CALCULATIONS
C*****
42 READ (5,100) (NN,NUM,S1,(K(J),J=1,NUM))
55 READ (5,101) (NO,L,LL,AR,(D(J),J=1,NUM))
FORMAT (2I2.7F10.0)
101 FORMAT (3I3.6F10.0)
C*****
C THE LAST DATA CARD MUST HAVE S1=200. TO TERMINATE THE JOB
C*****
43 IF(S1.GT.150.) GO TO 43
C*****
C WRITE SOME TITLES ON THE LINE PRINTER.
C ALSO WRITE THE DATA VALUES THAT HAVE JUST BEEN READ.
C*****
65 WRITE (6,I88)
188 FORMAT (1H,* TYPE OF SOURCE, NO. OF LAYERS, SIGMAL, AND SIGM/SIG
11 VALUES FROM BOTTOM UPWARDS #/)
WRITE (6,120) (NN,NUM,S1,(K(J),J=1,NUM))
120 FORMAT (2X,I2.6X,I2.4X,7(F14.6,2X)/)
C*****
70 WRITE (6,I91)
191 FORMAT (2X,* STN. NO., MODEL NO., MODEL SERIES NO., A/R VALUE AND
1 THICKNESSES FROM BOTTOM UPWARDS #/)
WRITE (6,124) (NO,L,LL,AR,(D(J),J=1,NUM))
124 FORMAT (2X,3I5.7(F14.7,2X)//)

```



\*\*\*\*\*  
 C HEADINGS FOR THE TWO TYPES OF DIPOLES  
 \*\*\*\*\*

```

IF (NN.NE.1) GO TO 288
WRITE (6,290)
FORMAT (4X, *CASE OF A HORIZONTAL MAGNETIC DIPOLE */)
WRITE (6,289)
FORMAT (14, *
      A      QDD      CS      REAL      DELTA      RF      QD
      I      REE      QDD      CS      REAL      QUAD */)
      GO TO 500
288 WRITE (6,291)
291 FORMAT (4X, * CASE OF A VERTICAL MAGNETIC DIPOLE */)
      WRITE (6,292)
292 FORMAT (14, *
      A      QDD      CS      DELTA      RF      QD
      I      REE      QDD */)
      GO 600 I=1,M
      B= X(I)
      A= AB*B
      PI2= PI*PI
      DEL= 25./R
  
```

\*\*\*\*\*  
 C NOW EQUAL TO 1 MEANS THAT WE ARE CONSIDERING THE CASE OF THE  
 C HORIZONTAL MAGNETIC DIPOLE  
 \*\*\*\*\*

```

IF (NN.NE.1) GO TO 489
TEF= 0
CALL CALC(TEE,A,R,D,K,CS,NUM,DEL,TREAL,TIMAG)
RE(I)= -TREAL
QD(I)= -TIMAG
TEF= 1
CALL CALC(TEE,A,R,D,K,CS,NUM,DEL,TREE,TIMM)
REE(I)= -TREE
QDD(I)= -TIMM
TEF= 2
CALL CALC(TEE,A,R,D,K,CS,NUM,DEL,TPE,TIM)
REAL(I)= -TRE
QUAD(I)= -TIM
  
```

115 C\*\*\*\*\*

C WRITE DOWN THE INTERMEDIATE VALUES THAT HAVE BEEN COMPUTED.

C\*\*\*\*\*

WRITE(6,579) A,CS,DEL,RE(I),QD(I),REE(I),QDD(I),REAL(I),QUAD(I)

579 FORMAT (2X,F8.4,4X,RE11.5)

120 RAL(I)= B\*\*3\*REE(I)

AIM1(I)= B\*\*3\*QDD(I)

RA2(I)= R\*R\*(REAL(I)-R\*RE(I))

AIM2(I)= B\*B\*(QUAD(I)-B\*QD(I))

GO TO 699

125 C\*\*\*\*\*

C NN EQUAL TO 2 MEANS THE CASE OF A VERTICAL MAGNETIC DIPOLE.

C\*\*\*\*\*

489 TEE= 0

CALL CALC(TEE,A,R,D,K,CS,NUM,DEL,TREAL,TIMAG)

RE(I)= -TREAL

QD(I)= -TIMAG

TEE= 1

130 C\*\*\*\*\*

CALL CALC(TEE,A,R,D,K,CS,NUM,DEL,TREE,TIMM)

REE(I)= -TREE

QDD(I)= -TIMM

135 C\*\*\*\*\*

C WRITE DOWN THE INTERMEDIATE VALUES THAT HAVE BEEN COMPUTED.

C\*\*\*\*\*

WRITE(6,589) A,CS,DEL,RE(I),QD(I),REE(I),QDD(I)

589 FORMAT (2X,F8.4,4X,6E11.5)

140 RAL(I)= B\*\*3\*REE(I)

AIM1(I)= B\*\*3\*QDD(I)

RA2(I)= R\*\*3\*REE(I)

AIM2(I)= B\*\*3\*QDD(I)

145 C\*\*\*\*\*

R1(I)= SORT(RA2(I)\*\*2\*AIM2(I)\*\*2)

R2(I)= SORT(RAL(I)\*\*2\*AIM1(I)\*\*2)

PH1(I)= ATAN2(AIM2(I),RA2(I))

PH2(I)= ATAN2(AIM1(I),RAL(I))

BLF(I)= 2.\*R1(I)\*R2(I)\*COS(PH2(I)-PH1(I))

150 C\*\*\*\*\*

C ALF= TILT ANGLE IN DEGREES

C\*\*\*\*\*

ALF(I)= 0.5\*ATAN2(BLF(I),(R1(I)\*\*2-R2(I)\*\*2))\*180./PIE

C\*\*\*\*\*

155 CLF(I) = 2.\*R1(I)\*R2(I)\*SIN(PH2(I)-PH1(I))/(R1(I)\*\*2+R2(I)\*\*2)  
BE12(I) = 0.5\*ASIN(CLF(I))  
C\*\*\*\*\*

C ELL = ELLIPTICITY OF THE FIELD.  
C\*\*\*\*\*

160 ELL(I) = ABS(TAN(BET2(I)))  
CONTINUE

879 WRITE (6,879)  
FORMAT (2X,\* GIVE A SMALL GAP\*//)

C\*\*\*\*\*

C WRITE THE FINAL COMPUTED VALUES  
C\*\*\*\*\*

199 WRITE (6,199)  
FORMAT (1H,\*  
1M2 R1 B R2 PA1 PH1 AIM1 PH2 RAP AI  
?LLI\*//)

170 WRITE (6,200) ((X(I),R1(I),A1(I),R2(I),AIM2(I),R1(I),R2(I),  
PH1(I),PH2(I),ALF(I),ELL(I)),I= 1,M)

200 FORMAT (2X,F6.3,4X,10F11.5)  
C\*\*\*\*\*

C INSTRUCTIONS TO GO TO STATEMENT 42 TO READ ANOTHER SET OF DATA  
C\*\*\*\*\*

GO TO 42

43 STOP  
ENJ)

175

SUBROUTINE CALC TRACE CDC 6400 FTN V3.0-P206 OPT=0 17/04/73 12.20.50.

SUBROUTINE CALC (TEE,A,B,D,K,CS,NUM,DEL,TREAL,TIMAG)
THIS SUBROUTINE CALCULATES THE INFINITE INTEGRALS I0,I1 AND I2.
THIS IS CALLED FROM THE MAIN PROGRAM COMP THREE TIMES FOR EACH

5 C DATA SET READ IN THE MAIN PROGRAM.
C DIMENSION P(10),Q(10),R(10),S(10)
REAL AW(96),W(96),X0(40),X1(40),AREAR(100),AREAI(100),7(100)
INTEGER TEE,L,I,M,N,N21,KI,JI
REAL A,B,EPS,MU,J,JWEX,J0X,J1X,KK
REAL Q(10),K(10)
LOGICAL BOOL
COMPLEX T(20),TA(20),PA(20),YA(20),PAA(20),PAB(20)
COMPLEX YE,PE,PF

15 C
C AW VALUES REPRESENT THE ABSCISSA VALUES X(I), WHERE X(I) IS THE ITH
C ZERO OF THE LEGENDRE POLYNOMIAL P\_N.
C W VALUES REPRESENT THE WEIGHT FACTORS W(I).
C X0 AND X1 ARE THE POSITIONS OF THE ZEROS OF THE BESSEL FUNCTIONS
C J0 AND J1. FORTY VALUES OF THEM HAVE BEEN CONSIDERED.

DATA AW / .99877100725, .99353017226, .98412458372, .97059159254,
A .95298770316, .93138669070, .90587913671, .87657202027,
B .84358826162, .80706620403, .76715903251, .72403413092,
C .67787237963, .62886739677, .57722472608, .52316097472,
D .46690290475, .40868648199, .34875588629, .28736248735,
E .22476379039, .16122235606, .09700469921, .03238017096,
I -.99877100725, -.99353017226, -.98412458372, -.97059159254,
2 -.95298770316, -.93138669070, -.90587913671, -.87657202027,
3 -.84358826162, -.80706620403, -.76715903251, -.72403413092,
4 -.67787237963, -.62886739677, -.57722472608, -.52316097472,
5 -.46690290475, -.40868648199, -.34875588629, -.28736248735,
6 -.22476379039, -.16122235606, -.09700469921, -.03238017096 /
DATA W / .00315334605, .00732755390, .01147723458, .01557931572,
A .01961616045, .02357076084, .02742650970, .03116722783,
B .0347722256, .03824135106, .04154508294, .04467456085,

C .04761665849, .05035903555, .05289018948, .05519950369,  
 D .05727729210, .05911483969, .06070443916, .06203942316,  
 E .06311419228, .06392423858, .06446616443, .06473769681,  
 1 .00315334605, .00732755390, .01147723458, .01557931572,  
 2 .01961616045, .02357076084, .02742650970, .03116722783,  
 3 .0347722256, .03824135106, .04154508294, .04467456085,  
 4 .04761665849, .05035903555, .05289018948, .05519950369,  
 5 .05727729210, .05911483969, .06070443916, .06203942316,  
 6 .06311419228, .06392423858, .06446616443, .06473769681 /

40

DATA X0/2,404825577,5.52007811038,6537279129,11.791534439,  
 1 14.939017708,18.071063968,21.211636630,24.352471531,  
 2 27.493479132,30.634606468,33.775820214,36.917098354,  
 3 40.058425755,43.199791713,46.341188372,49.482609897,  
 4 52.624051841,55.765510755,58.906983926,62.048469190,  
 5 65.189964868,68.3314693,71.4729816,74.6145006,77.7560256,  
 6 80.8975559,84.0390908,87.1806298,90.3221726,93.4637188,  
 7 96.6052680,99.7468199,102.8893743,106.0299309,109.1714896,  
 8 112.3130503,115.4546127,118.5961766,121.7377421,124.8793089/  
 DATA X1/3,83170597,7.01558667,10.17346814,13.32369194,16.47063005,  
 1 19.61585851,22.76008438,25.90367209,29.04682853,32.18967991,  
 2 35.33230755,38.47476623,41.61709421,44.75931900,47.90145089,  
 3 51.04353518,54.18555364,57.32752544,60.46945785,63.61135670,  
 4 66.7532267,69.89950718,73.0368952,76.1786996,79.3204872,  
 5 82.4622599,85.6040194,88.7457671,91.8875043,95.0292318,  
 6 98.1709507,101.3126614,104.4543658,107.5960633,110.7377548,  
 7 113.8794408,117.0211219,120.1627983,123.3044705,126.4461387/  
 DATA M,N/48,40/

50

55  
 50  
 55

55  
 50  
 55

C \*\*\*\*\*  
 C CHECK INPUTS HERE \*\*\*\*\*  
 C M IS THE NUMBER OF SUBDIVISIONS WITHIN THE AREA ROUNDED BY TWO \*\*\*\*\*  
 C CONSECUTIVE ZEROS OF THE BESSEL FUNCTION AND N IS THE NUMMR \*\*\*\*\*  
 C OF SUCH SEGMENTS. \*\*\*\*\*  
 C \*\*\*\*\*

70

C IF (TEE.LT.0.OR.TEE.GT.2.OR.B.FQ.0.OR.A.EQ.0) RETURN  
 L=1

```
75 IF (TFE.EQ.0) GO TO 60
   DO 50 I=1,N
   Z(I) = X1(I)/R
50  GO TO 90
C
R0 DO 70 I=1,N
   Z(I) = X0(I)/R
C
90 CONTINUE
SUMR=0.
SUMI=0.
IF (L.F.O.1) GO TO 95
GL=60
SU=Z(L)
GO TO 9R
95 GL=0.
GU=Z(1)
MU=.5*(GU-GL)
C
95 C***** CALL FUNCTION GG *****
   DO 900 I=1,M
   G=GG(AW(I),SU,GL)
   GP= G*G
   G4=G2*G2
   GY= G*A
   IF (GY .GE. 700.) GY = 680.
   EX= EXP(-GY)
   IF (EX .LT. 1.E-35) EX= 0.0
   IF (ABS(G) .LT. 1.F-10) STOP 2
   DO 200 JI= 1,NUM
   KK= K(JI)
   DD=D(JI)/DEL
   U= SORT(S4+4.*KK*KK)
   ALP= SORT(.5*(G2+JI))
   RFT= KK/ALP
   P(JI)= BET/CS
```

110

```
115 Q(JI)=-ALP/CS
    PA(JI)=CMPLX(P(JI),0.(JI))
    IF (JI.F0.1) GO TO 200
    R(JI)=2.*DD*ALP
    S(JI)=2.*DD*RET
    T(JI)=CMPLX(R(JI),S(JI))
    TA(JI)=(1.-CEXP(-T(JI)))/(1.+CEXP(-T(JI)))
    CONTINUE
    200 DO 250 KI=1,NUM
        IF (KI.NE.1) GO TO 86
        YA(KI)=PA(KI)
        GO TO 250
    86 PAA(KI)=PA(KI)*TA(KI)
        PAR(KI)=YA(KI-1)*TA(KI)
        YA(KI)=PA(KI)*(YA(KI-1)+PAA(KI))/(PA(KI)+PAR(KI))
    250 CONTINUE
    YE=YA(NUM)
    PE=CMPLX(0,0,-G/CS)
    RF=(PE-YE)/(PE+YE)
    RU=REAL(RF)
    RI=AIMAG(RF)
    GO TO 500
*****
135 C COMPUTATION OF THE INTEGRAL
    C *****
    600 H=H*G
    WEX=W(I)*EX
    IF (TEE.NE.0) GO TO 650
    C ***** CALL FUNCTION J0X *****
    J=J0X(H)*G2
    GO TO 800
    650 IF (TEE.NE.1) GO TO 700
    C ***** CALL FUNCTION J1X *****
    J=J1X(H)*G2
    GO TO 800
    C ***** CALL FUNCTION J1X *****
    700 J=J1X(H)*G
    800 JWEX=J*WEX
    SUMR=SUMR+RD*JWEX
    C ***** CALL FUNCTION J1X *****
```

```
150 SUMI=SUMI+RI*JWEX
    CONTINUE
    900 AREAR(L)=MU*SUMR
        AREAI(L)=MU*SUMI
        IF (L.GE.3) GO TO 1100
        EPS=1.E-06
        ER= ABS(AREAR(L))*EPS
    EI= ABS(AREAI(L))*EPS
    TR2= ABS(AREAR(L))
    TI2= ABS(AREAI(L))
    950 CONTINUE
    L=L+1
    GO TO 90
1100 TR1=TR2
    TI1=TI2
    TR2= ABS(AREAR(L))
    TI2= ABS(AREAI(L))
    ROOT=(TR2.GT.TR1).OR.(TI2.GT.TI1)
    IF (.NOT.(ROOT.AND.(L.EQ.N))) GO TO 1200
    L=N
    GO TO 2000
1200 IF (ROOT) GO TO 950
    ROOT=(TR2.GE.ER).OR.(TI2.GE.EI)
    IF (.NOT.(ROOT.AND.(L.EQ.N))) GO TO 1300
    L=1000000
    GO TO 2000
1300 IF (ROOT) GO TO 950
    SUR=0.
    SUI=0.
    DO 1400 I=1,L
    SUR=SUR+AREAR(I)
    SUI=SUI+AREAI(I)
1400 CONTINUE
    TREAL=SUR
    TIMAG=SUI
```



```

185 C***** RETURN *****
      RETURN
      2000 CONTINUE
C***** CALL SURROUTINE *****
190 CALL EULER (N/2,N,AREAR,EUSUR)
      C***** CALL SURROUTINE *****
      CALL EULER (N/2,N,ARFAT,EUSUI)
      SUR=0.
      SUI=0.
      N21=N/2-1
      00 2200 I=1,N21
      SUR=SUR+AREAR(I)
      SUI=SUI+AREAI(I)
      2200 CONTINUE
      SUR=SUR+EUSUR
      SUI=SUI+EUSUI
      WRITE (6,599) TEE,EUSUR,EUSUI,SUR,SUI
      599 FORMAT (2X,I2,2X,4E15.8)
      TREAL=SUR
      TIMAG=SUI
C***** RETURN *****
205 RETURN
      END

```

SUBROUTINE EULER TRACE CDC 6400 FTN V3.0-P296 OPT=0 17/04/73 12.20.50.

SUBROUTINE EULER (M,N,7,SUM)
C \*\*\*\*\*
C THIS SUBROUTINE FINDS THE EULER'S SUMMATION WHEN THE INTEGRAL DOES
C NOT CONVERGE AFTER 20 SEGMENTS.

5 C IT IS CALLED FROM THE SUBROUTINE CALC TWICE AFTER STATEMENT NUMBER 2000.
C \*\*\*\*\*
REAL Z(40),B(100),SUM,FAC
C \*\*\*\*\*
IF (M.GT.N.OR.M.LE.0) RETURN
K = N-M+1

10 L = M-1
SUM = 0.
DO 10 I=1,K,2
10 R(I) = Z(L+I)
DO 20 I=2,K,2
20 B(I) =-Z(L+I)
KP=K+1

DO 40 I=2,K
KM=KP-I
DO 30 J=1,KM
K1=KP-J
30 B(K1) =-B(K1-1) + R(K1)
40 CONTINUE

FAC = .5
DO 50 I=1,K
SUM = SUM + FAC\*B(I)
25 FAC = .5\*FAC
50
C \*\*\*\*\* RETURN \*\*\*\*\*
RETURN

30 END

FUNCTION J0X TRACE CDC 6400 FTN V3.0-P206 OPT=0 17/04/73 12.20.50.

REAL FUNCTION J0X(X)
C \*\*\*\*\*
C THIS SUBROUTINE COMPUTES THE BESSEL FUNCTION J0.
C IT IS CALLED FROM THE SURROUTINE\_CALC 4 LINES AFTER THE STATEMENT

5 C NUMBER 600.
C \*\*\*\*\*
C REAL X,T,Y,FO,PHO
C \*\*\*\*\*
C TEST FOR THE TWO DIFFERENT PATHS THAT MAY BE FOLLOWED.
C \*\*\*\*\*

10 IF (X.GT.3.) GO TO 10
T=X/3.
Y=T\*T
J0X = 1.-Y\*(2.249997-Y\*(1.2656208-Y\*(.3163866-Y\*(.0444479-Y\*
(3.9444E-3-2.1E-4\*Y))))))

15 RETURN
C \*\*\*\*\* RETURN \*\*\*\*\*
10 Y=3./X
FO = .7978456-Y\*(7.7E-7+Y\*(.55274E-2+Y\*(.9512E-4-Y\*
(.137237E-2-Y\*(.72805E-3-.14476E-3\*Y))))))
20 PHO = .7853981+Y\*(.04166397+Y\*(.3954E-4-Y\*(.00262573-Y\*
(.54125E-3+Y\*(.29333E-3-.1355AE-3\*Y))))))

J0X = SQRT(1./X)\*FO\* COS(X-PHO)
\*\*\*\*\* RETURN \*\*\*\*\*
25 RETURN
END

FUNCTION J1X TRACE CDC 6400 FTN V3.0-P206 OPT=0 17/04/73 12.20.50.

REAL FUNCTION J1X(X) \*\*\*\*\*  
C THIS SUBROUTINE COMPUTES THE BESSEL FUNCTION J1.  
C IT IS CALLED FROM THE SUBROUTINE CALC 1 LINE AFTER STATEMENT NUMBER 650 \*\*\*\*\*

5 C AND AT STATEMENT NUMBER 700. \*\*\*\*\*

REAL X,Y,T,FI,PHI \*\*\*\*\*  
C TEST FOR THE TWO DIFFERENT PATHS THAT MAY BE FOLLOWED. \*\*\*\*\*  
C \*\*\*\*\*

10 IF (X.GT.3.) GO TO 10 \*\*\*\*\*  
T = X/3. \*\*\*\*\*  
Y = T\*T \*\*\*\*\*  
J1X = X\*(.5-Y\*(.56249945-Y\*(.21093573-Y\*(.03954289-Y\*  
(.00443319-Y\*(.31761E-3-.1109E-4\*Y)))) \*\*\*\*\*  
C \*\*\*\*\* RETURN \*\*\*\*\*

RETURN \*\*\*\*\*  
10 Y = 3./X \*\*\*\*\*  
FI = .79788456+Y\*(.156E-5+Y\*(.01659667+Y\*(.17105E-3-Y\*  
(.00249511-Y\*(.00113653-.20033E-3\*Y)))) \*\*\*\*\*  
20 PHI = .78539416-Y\*(.12499612+Y\*(.5650E-4-Y\*(.00637879-Y\*  
(.74348E-3+Y\*(.79824E-3-.29166E-3\*Y)))) \*\*\*\*\*

J1X = SQRT(1./X)\*FI\* SIN(X-PHI) \*\*\*\*\*  
RETURN \*\*\*\*\*  
25 END \*\*\*\*\*

FUNCTION G6 TRACE CDC 6400 FTN V3.0-P296 OPT=0 17/04/73 12.20.50.

FUNCTION G6 (X,GU,GL)
C \*\*\*\*\*
C THIS SUBROUTINE CALCULATES THE VARIABLE G FOR USE IN GAUSSIAN QUADRATURE.
C IT IS CALLED FROM THE SUBROUTINE CALC 2 LINES AFTER STATEMENT NUMBER 98.
C \*\*\*\*\*

5 REAL X,GU,GL
GG = .5\*(X\*(GU-GL)+GL\*GU)
C \*\*\*\*\* RETURN \*\*\*\*\*
RETURN
EN)
10

TYPE OF SOURCE, NO. OF LAYERS, SIGNAL, AND SIGMA/SIGI VALUES FROM BOTTOM UPWARDS

1 3 .100000 .010000 .100000 1.000000  
 STN. NO., MODEL NO., MODEL SERIES NO., A/R VALUE AND THICKNESSES FROM BOTTOM UPWARDS

1 3 1 4.0000000 0.0000000 15.0000000 10.0000000  
 CASE OF A HORIZONTAL MAGNETIC DIPOLE.

A	CS	DELTA	RE	QD	REE	ODD	REAL	PH2	ALPHA	ELLI	
.4000	.8000E+00	.25000E+03	.54979E-02	.21955E-02	.50326E-03	.64856E-01	.27840E-03	.11389E-01	.15604E+01	.24455E+02	.57980E-02
.4880	.37600E-01	.20492E+03	.63808E-02	.17955E+00	.61098E-03	.39790E-01	.39335E-03	.11354E-01	.15554E+01	.24700E+02	.80278E-02
.6000	.12000E+00	.16467E+03	.74125E-02	.14535E-02	.74599E-03	.32340E-01	.56133E-03	.11307E-01	.15477E+01	.24777E+02	.11168E-01
.7200	.14400E+00	.13889E+03	.84027E-02	.12032E+00	.88725E-03	.26916E-01	.76439E-03	.11234E-01	.15378E+01	.24877E+02	.14775E-01
.8920	.17840E+00	.11211E+03	.96231E-02	.95871E-01	.10817E-02	.21663E-01	.10857E-02	.11095E-01	.15209E+01	.25052E+02	.20282E-01
1.0880	.21760E+00	.91912E+02	.10735E-01	.77951E-01	.12889E-02	.17664E-01	.14786E-02	.10884E-01	.14980E+01	.25298E+02	.26786E-01
1.3400	.26800E+00	.74627E+02	.11757E-01	.60463E-01	.15277E-02	.14184E-01	.19972E-02	.10530E-01	.14635E+01	.25674E+02	.35096E-01
1.6320	.32640E+00	.61275E+02	.12433E-01	.47152E-01	.17592E-02	.1417E-01	.25768E-02	.10019E-01	.14179E+01	.26179E+02	.44234E-01
1.9800	.39600E+00	.50505E+02	.12454E-01	.35976E-01	.19660E-02	.90920E-02	.31893E-02	.92972E-02	.13578E+01	.26547E+02	.56025E-01
2.4600	.48800E+00	.40984E+02	.12240E-01	.25751E-01	.21250E-02	.69179E-02	.38146E-02	.82341E-02	.12728E+01	.27791E+02	.64783E-01
3.0000	.52000E+00	.33333E+02	.11094E-01	.17661E-01	.21658E-02	.50605E-02	.42705E-02	.69049E-02	.11664E+01	.28965E+02	.74483E-01
3.6000	.72000E+00	.27778E+02	.95517E-02	.11666E-01	.20733E-02	.36558E-02	.44348E-02	.55754E-02	.10549E+01	.30187E+02	.81137E-01
4.4000	.88000E+00	.22727E+02	.75101E-02	.69247E-02	.18286E-02	.23845E-02	.42915E-02	.40862E-02	.91658E+00	.31682E+02	.85145E-01
5.4400	.10880E+01	.18342E+02	.53249E-02	.36142E-02	.14510E-02	.13895E-02	.37946E-02	.26755E-02	.76050E+00	.33334E+02	.84461E-01
6.7200	.13440E+01	.14881E+02	.34650E-02	.17167E-02	.10393E-02	.72114E-03	.30784E-02	.15925E-02	.60651E+00	.34901E+02	.78383E-01
8.2000	.16400E+01	.12195E+02	.21646E-02	.78841E-03	.69553E-03	.35750E-03	.23614E-02	.90557E-03	.50379E-02	.25643E+01	.60651E+00
10.0000	.20000E+01	.10000E+02	.12854E-02	.34727E-03	.43517E-03	.16650E-03	.17249E-02	.49244E-03	.42915E-02	.28965E+02	.74483E-01
12.2000	.24400E+01	.81947E-01	.74141E-03	.15202E-03	.25934E-03	.75345E-04	.12197E-02	.26523E-03	.10549E+01	.30187E+02	.81137E-01
15.0000	.30000E+01	.66667E+01	.41224E-03	.46590E-04	.14730E-03	.33535E-04	.83677E-03	.14347E-03	.14635E+01	.25674E+02	.35096E-01
GIVE A SMALL GAP											
B	RA1	AIM1	RAP	AIM2	R1	R2	PH1	PH2	ALPHA	ELLI	
.100	.50326E-06	.48560E-04	.27139E-05	.10574E-03	.10579E-03	.48563E-04	.15965E+01	.15604E+01	.24455E+02	.57980E-02	
.122	.11094E-05	.72253E-04	.57319E-05	.16498E-03	.15708E-03	.72262E-04	.14073E+01	.15554E+01	.24700E+02	.80278E-02	
.150	.25177E-05	.10915E-03	.12387E-04	.23614E-03	.23367E-03	.10918E-03	.16232E+01	.15477E+01	.24777E+02	.11168E-01	
.180	.51744E-05	.15698E-03	.24238E-04	.33769E-03	.33845E-03	.15706E-03	.16425E+01	.15378E+01	.24877E+02	.14775E-01	
.223	.11955E-04	.24023E-03	.52726E-04	.51143E-03	.24053E-03	.16735E-03	.17129E+01	.15209E+01	.25052E+02	.20282E-01	
.272	.25937E-04	.35547E-03	.10664E-03	.74534E-03	.75293E-03	.35641E-03	.17129E+01	.14980E+01	.25298E+02	.26786E-01	
.335	.57336E-04	.53324E-03	.21787E-03	.10913E-02	.11129E-02	.53632E-03	.17678E+01	.14635E+01	.25674E+02	.35096E-01	
.408	.11948E-03	.77544E-03	.61565E-03	.15342E-02	.15900E-02	.78459E-03	.19352E+01	.14179E+01	.26179E+02	.44234E-01	
.495	.23845E-03	.11028E-02	.75327E-03	.20845E-02	.22173E-02	.11828E-02	.19178E+01	.13578E+01	.26547E+02	.56025E-01	
.610	.48233E-03	.15702E-02	.13588E-02	.27811E-02	.30953E-02	.16427E-02	.20253E+01	.12728E+01	.27791E+02	.64783E-01	
.750	.91368E-03	.21349E-02	.22783E-02	.34424E-02	.41614E-02	.23222E-02	.21501E+01	.11664E+01	.28965E+02	.74483E-01	
.900	.15115E-02	.26651E-02	.33710E-02	.39886E-02	.52224E-02	.30939E-02	.27255E+01	.10549E+01	.30187E+02	.81137E-01	
1.100	.24339E-02	.31738E-02	.48032E-02	.47272E-02	.64285E-02	.39966E-02	.26146E+01	.91658E+00	.31682E+02	.85145E-01	
1.360	.36499E-02	.34726E-02	.63760E-02	.41527E-02	.76050E-02	.50379E-02	.25643E+01	.76050E+00	.33334E+02	.84461E-01	
1.680	.49279E-02	.44194E-02	.77412E-02	.36453E-02	.85566E-02	.59880E-02	.27017E+01	.60651E+00	.34901E+02	.78383E-01	
2.050	.59821E-02	.30799E-02	.86889E-02	.24866E-02	.91878E-02	.67373E-02	.26105E+01	.47478E+00	.36166E+02	.88618E-01	
2.500	.67995E-02	.26016E-02	.93038E-02	.23480E-02	.95955E-02	.72802E-02	.28444E+01	.36543E+00	.37136E+02	.56976E-01	
3.050	.73582E-02	.21377E-02	.96491E-02	.18459E-02	.98633E-02	.76624E-02	.29533E+01	.28274E+00	.37812E+02	.45800E-01	
3.750	.77678E-02	.17684E-02	.99747E-02	.14940E-02	.10086E-01	.79665E-02	.29929E+01	.22385E+00	.38286E+02	.36581E-01	

TYPE OF SOURCE, NO. OF LAYERS, SIGNAL, AND SIGM/SIG1 VALUES FROM BOTTOM UPWARDS

STN. NO., MODEL NO.,	MODEL SERIES NO.,	A/R VALUE	AND THICKNESSES FROM BOTTOM UPWARDS	CS	DELTA	RE	OD	REE	R2	PH1	PH2	ALPHA	ELLI
2	2	6.0000000	0.0000000	15.0000000	10.0000000	10.0000000	10.0000000	10.0000000	10.0000000	10.0000000	10.0000000	10.0000000	10.0000000
CASE OF A VERTICAL MAGNETIC DIPOLE													
6000		.90000E+00	.25000E+03	.50242E+00	.11019E+01	.46870E-01	.17006E+00						
7320		.37680E+00	.20492E+03	.44522E+00	.77595E+00	.45984E-01	.12911E+00						
9000		.12000E+01	.16667E+03	.37432E+00	.51212E+00	.44801E-01	.91518E-01						
10800		.14400E+01	.13889E+03	.30600E+00	.33655E+00	.40771E-01	.64881E-01						
13300		.17840E+01	.11211E+03	.22601E+00	.19077E+00	.33885E-01	.40339E-01						
16320		.21740E+01	.9191E+02	.15942E+00	.10425E+00	.26352E-01	.23973E-01						
20100		.26800E+01	.74827E+02	.10321E+00	.51171E-01	.18587E-01	.12738E-01						
24800		.32640E+01	.61753E+02	.65625E-01	.24614E-01	.12390E-01	.65127E-02						
29700		.39600E+01	.50505E+02	.39198E-01	.11684E-01	.78523E-02	.32276E-02						
34600		.48800E+01	.40944E+02	.22170E-01	.52813E-02	.45832E-02	.15016E-02						
40500		.60000E+01	.33333E+02	.12435E-01	.25328E-02	.26239E-02	.73216E-03						
54000		.72000E+01	.27778E+02	.74426E-02	.13956E-02	.15929E-02	.40805E-03						
68000		.88000E+01	.22127E+02	.42363E-02	.75512E-03	.91997E-03	.22373E-03						
81600		.10880E+02	.18382E+02	.23391E-02	.40457E-03	.51594E-03	.12170E-03						
100800		.13440E+02	.14881E+02	.12970E-02	.22107E-03	.29065E-03	.67543E-04						
123000		.16400E+02	.12195E+02	.74671E-03	.12569E-03	.17004E-03	.39002E-04						
150000		.20000E+02	.10000E+02	.43214E-03	.69972E-04	.10014E-03	.22085E-04						
183000		.24400E+02	.81967E+01	.24974E-03	.36941E-04	.58918E-04	.11867E-04						
225000		.30000E+02	.66667E+01	.14034E-03	.17742E-04	.33666E-04	.57966E-05						
GIVE A SMALL GAP													
B	RAI	AIM1	RAP	ATM2	RI	R2	PH1	PH2	ALPHA	ELLI			
.100	.50242E-03	.11019E-02	.46870E-04	.17006E-03	.17641E-03	.12110E-02	.13019E+01	.11430E+01	.81811E+02	.22578E-01			
.122	.80845E-03	.14090E-02	.85317E-04	.23263E-03	.24778E-03	.16245E-02	.12193E+01	.10499E+01	.81444E+02	.25146E-01			
.150	.12533E-02	.1728E-02	.15120E-03	.30887E-03	.34300E-03	.21409E-02	.11156E+01	.93961E+00	.81006E+02	.27429E-01			
.180	.17846E-02	.19628E-02	.23778E-03	.37939E-03	.44689E-03	.26528E-02	.10098E+01	.83291E+00	.80576E+02	.28843E-01			
.223	.25063E-02	.21156E-02	.37577E-03	.44735E-03	.58423E-03	.32398E-02	.8721E+00	.70106E+00	.80036E+02	.29418E-01			
.272	.32081E-02	.20980E-02	.53030E-03	.44242E-03	.71690E-03	.38332E-02	.73816E+00	.57916E+00	.79529E+02	.28638E-01			
.335	.38801E-02	.19238E-02	.69877E-03	.47889E-03	.84712E-03	.43308E-02	.60081E+00	.46029E+00	.79031E+02	.26404E-01			
.408	.43891E-02	.16717E-02	.84151E-03	.44233E-03	.95068E-03	.46967E-02	.44394E+00	.36392E+00	.78631E+02	.23295E-01			
.495	.47399E-02	.1171E-02	.95238E-03	.39147E-03	.10297E-02	.49606E-02	.34999E+00	.28971E+00	.78326E+02	.19930E-01			
.610	.50321E-02	.11988E-02	.10403E-02	.34083E-03	.1097E-02	.51729E-02	.31660E+00	.23386E+00	.78088E+02	.16745E-01			
.750	.52858E-02	.10685E-02	.10170E-02	.30883E-03	.11492E-02	.53536E-02	.27211E+00	.20094E+00	.77911E+02	.14596E-01			
.900	.54256E-02	.10174E-02	.11412E-02	.29747E-03	.11987E-02	.55202E-02	.25078E+00	.18536E+00	.77772E+02	.13550E-01			
1.100	.56385E-02	.10051E-02	.12245E-02	.29778E-03	.12602E-02	.57274E-02	.23856E+00	.17640E+00	.77412E+02	.13039E-01			
1.360	.58840E-02	.10177E-02	.12978E-02	.30613E-03	.13334E-02	.59713E-02	.23165E+00	.17126E+00	.77432E+02	.12838E-01			
1.680	.61499E-02	.10492E-02	.13782E-02	.32026E-03	.14149E-02	.62386E-02	.22833E+00	.16883E+00	.77241E+02	.12830E-01			
2.050	.64330E-02	.10828E-02	.14669E-02	.33601E-03	.15029E-02	.65235E-02	.22547E+00	.16676E+00	.77045E+02	.12840E-01			
2.500	.67521E-02	.10933E-02	.15446E-02	.34507E-03	.16022E-02	.68401E-02	.21707E+00	.16053E+00	.76835E+02	.12551E-01			
3.050	.70859E-02	.10481E-02	.16171E-02	.36471E-03	.17630E-02	.71630E-02	.19876E+00	.14685E+00	.76625E+02	.11692E-01			
3.750	.74008E-02	.93562E-03	.17755E-02	.30568E-03	.18016E-02	.74597E-02	.17050E+00	.12575E+00	.76934E+02	.10208E-01			